UNIVERSITY OF SURREY

Recent Advances in SCGF Calculations

Carlo Barbieri — University of Surrey

2 March 2017

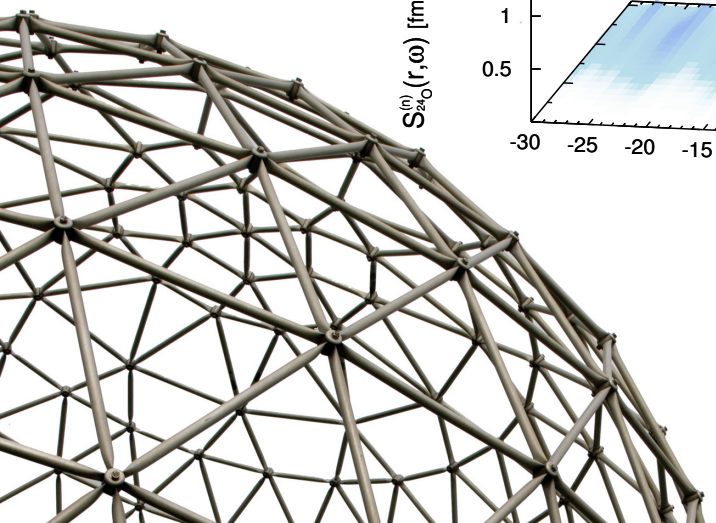

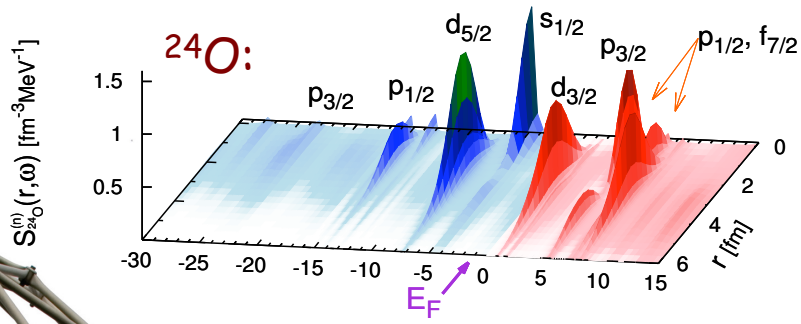

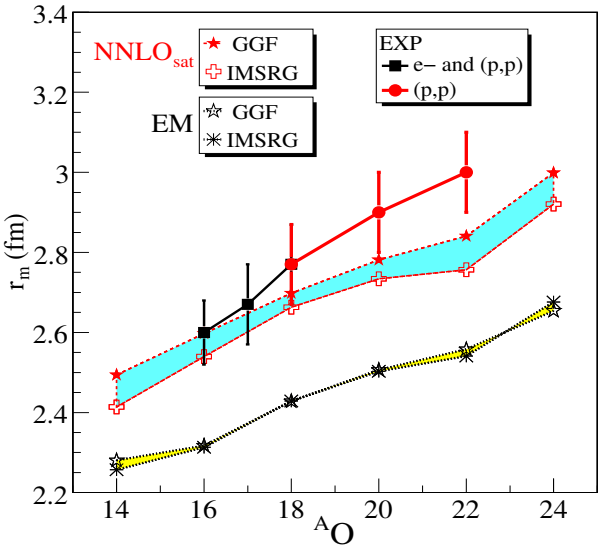

Outilne

- *Some details of the current SCGF formalism (extensions for 3NFs)*
- *Application of saturating interactions and new local-nonlocal force*
- *Bubble structure of ^{34}Si*
- *occupation of valence shells*
- *Nuclei from Lattice QCD (at m_π=0.47 GeV/c^2 ...)*

Related calculations (see following talks):

- *Shell model effective charges*
- *Dipole response*
- *Ab-Initio optical potential from SCGF*

Current Status of low-energy nuclear physics

Composite system of interacting fermions

Binding and limits of stability

Coexistence of individual and collective behaviors

Self-organization and emerging phenomena

EOS of neutron star matter

Experimental programs
RIKEN, FAIR, FRIB

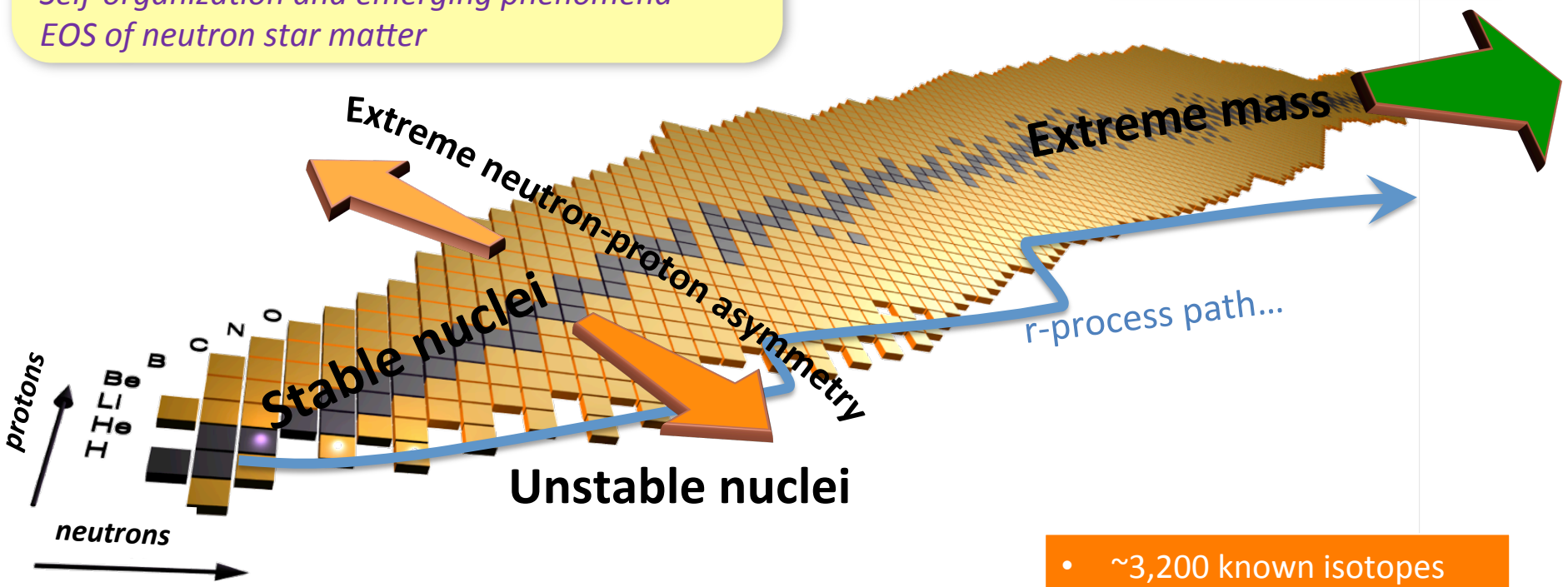

- ~3,200 known isotopes
- ~7,000 predicted to exist
- Correlation characterised in full for ~283 stable

Nature **473**, 25 (2011); **486**, 509 (2012)

The FRPA Method in Two Words

Particle vibration coupling is the main cause driving the distribution of particle strength—on both sides of the Fermi surface…

CB et al.,
*Phys. Rev. C**63**, 034313 (2001)*
*Phys. Rev. A**76**, 052503 (2007)*
*Phys. Rev. C**79**, 064313 (2009)*

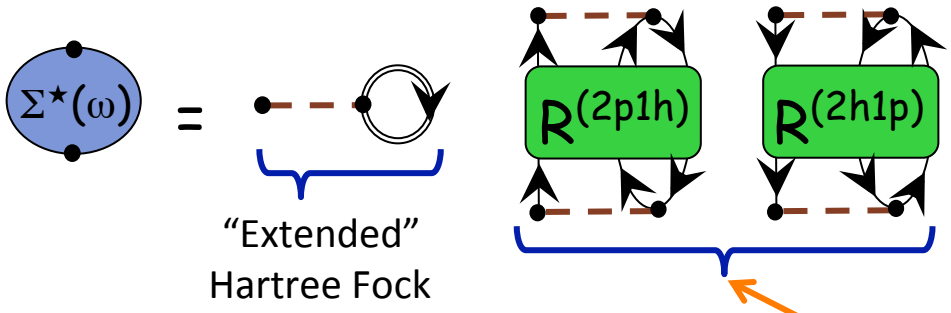

- A complete expansion requires *all types* of particle-vibration coupling

  …these modes are all resummed exactly and to all orders in a *ab-initio* many-body expansion.

- The Self-energy $\Sigma^{\star}(\omega)$ yields *both* single-particle states and scattering

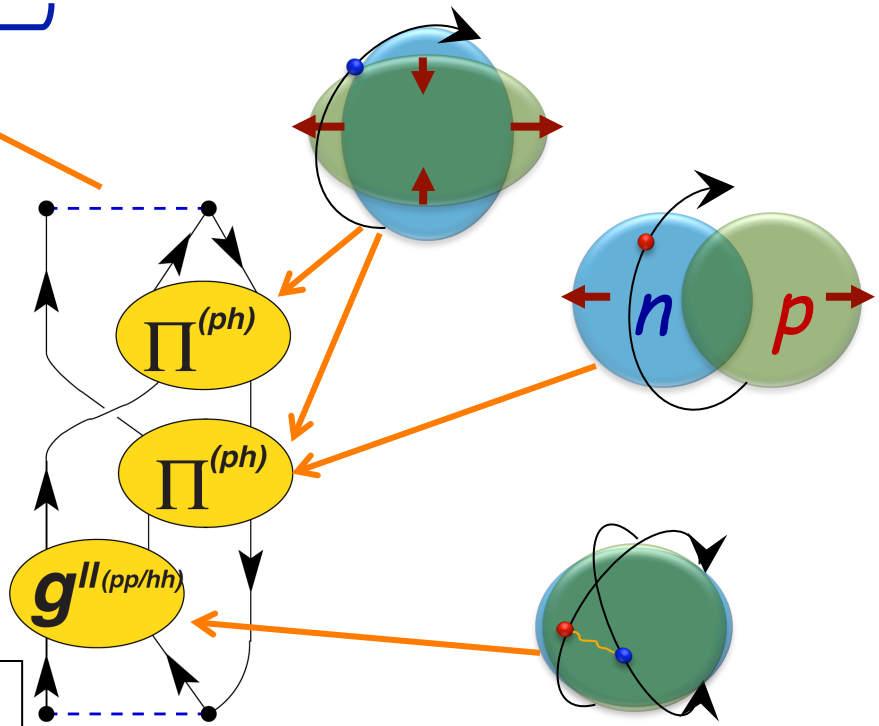

Self-Consistent Green's Function Approach

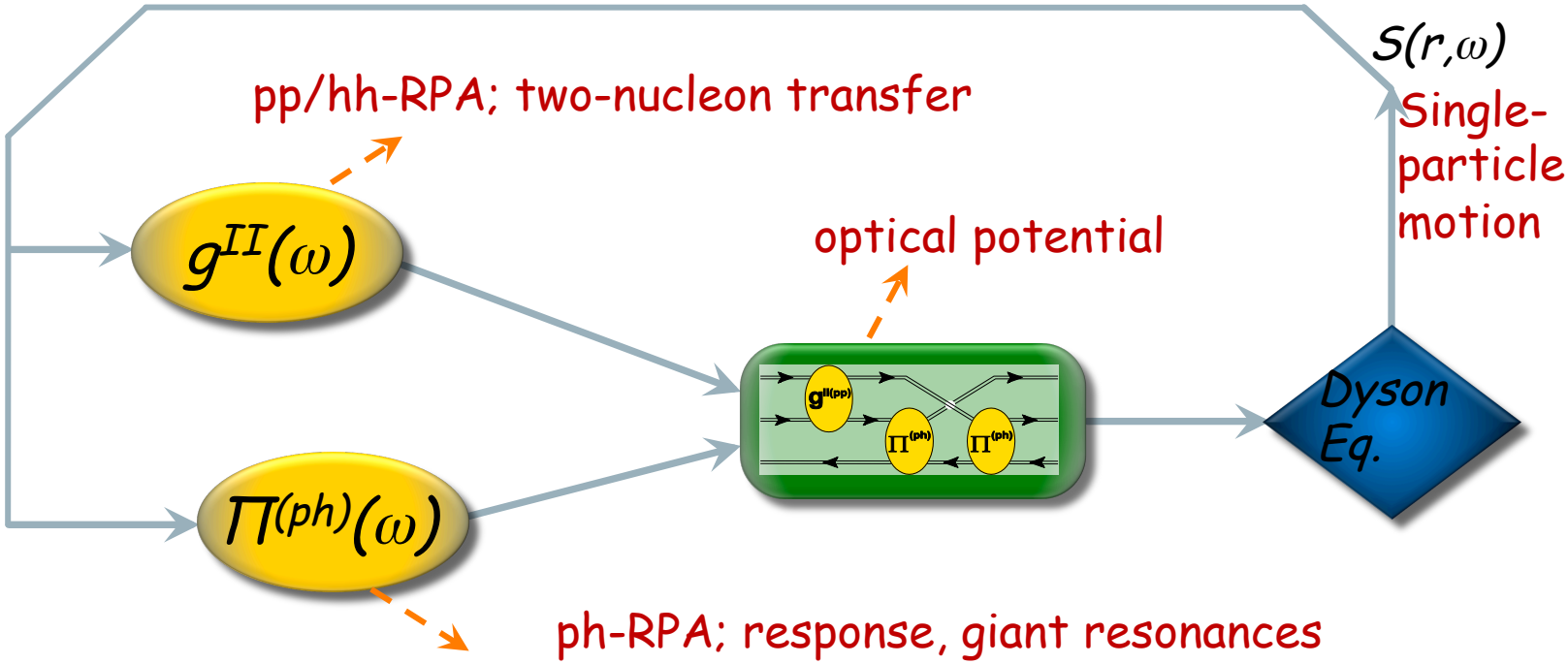

- Global picture of nuclear dynamics
- Reciprocal correlations among effective modes
- Guaranties *macroscopic conservation laws*

Self-Consistent Green's Function Approach

^{16}O(e,e'pn)^{14}N @ MAINZ

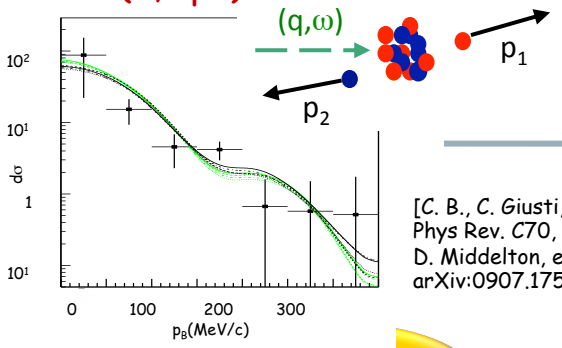

[C. B., C. Giusti, et al.
Phys Rev. C70, 014606 (2004)
D. Middelton, et al.
arXiv:0907.1758; EPJA in print]

Binding energies

[PRL. 111, 062501 (2013),
PRC 92, 014306 (2015), PRC89, 061301R (2014)]

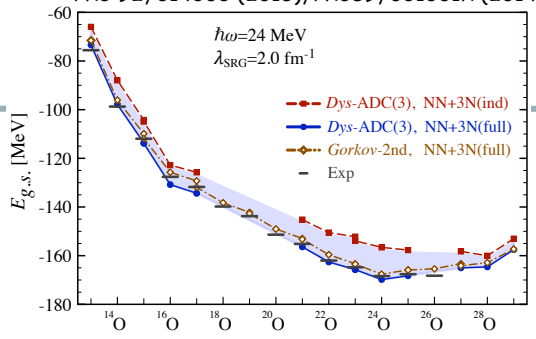

Ionization energies/ affinities, in atoms

[CB, D. Van Neck,
AIP Conf.Proc.1120,104 ('09) & in prep]

		Hartree-Fock	FRPAc	Experiment [16, 17]
He:	1s	0.918 (+14)	0.9008 (-2.9)	0.9037
Be^{2+}:	1s	5.6672 (+116)	5.6551 (-0.5)	5.6556
Be:	2s	0.3093 (-34)	0.3224 (-20.2)	0.3426
	1s	4.733 (+200)	4.5405 (+8)	4.533
Ne:	2p	0.852 (+57)	0.8037 (+11)	0.793
	1s	1.931 (+149)	1.7967 (+15)	1.782
Mg^{2+}:	2p	3.0068 (+56.9)	2.9537 (+3.8)	2.9499
	1s	4.4827	4.3589	
Mg:	3s	0.253 (-28)	0.280 (-1)	0.281
	2p	2.282 (+162)	2.137 (+17)	2.12
Ar:	3p	0.591 (+12)	0.579 (≈0)	0.579
	3s	1.277 (+202)	1.065 (-10)	1.075
	3s		1.544	
	2p	9.571 (+411)	9.219 (+59)	9.160

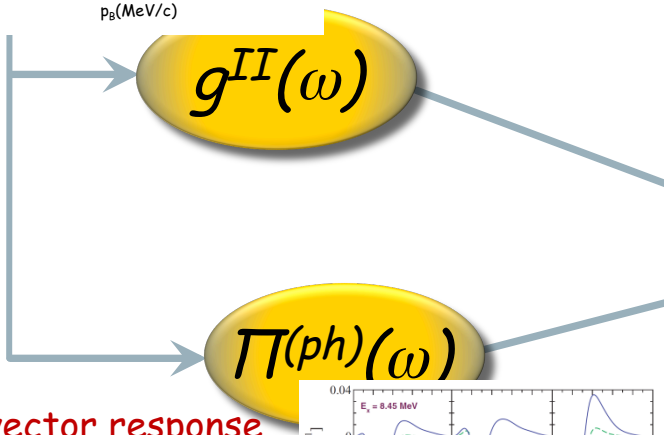

Isovector response for ^{32}Ar, ^{34}Ar

Proton Pygmy

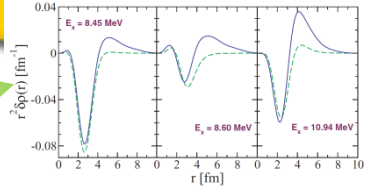

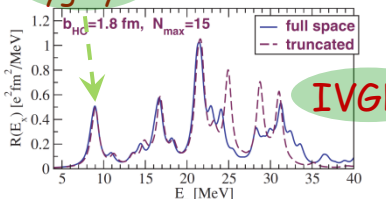

IVGDR

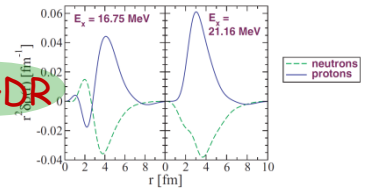

[C. B., K. Langanke, et al., Phys Rev. C77, 024304 (2008)]

Optical potential (see talk by A. Idini)

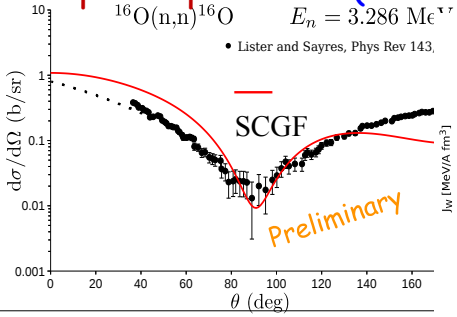

arXiv:1612.01478 [nucl-th]

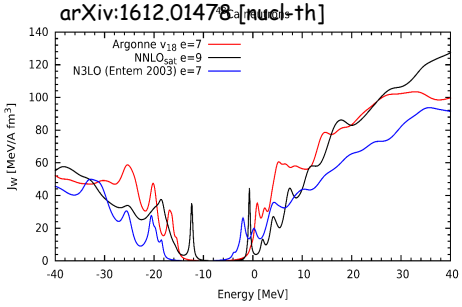

Gorkov
and
3-nucleon forces

Approaches in GF theory

Truncation scheme:	Dyson formulation (closed shells)	Gorkov formulation (semi-/doubly-magic)
1st order:	Hartree-Fock	HF-Bogolioubov
2nd order:	2nd order	2nd order (w/ pairing)
. . .	. . .	
3rd and all-orders sums, P-V coupling:	ADC(3) FRPA etc…	G-ADC(3) …work in progress

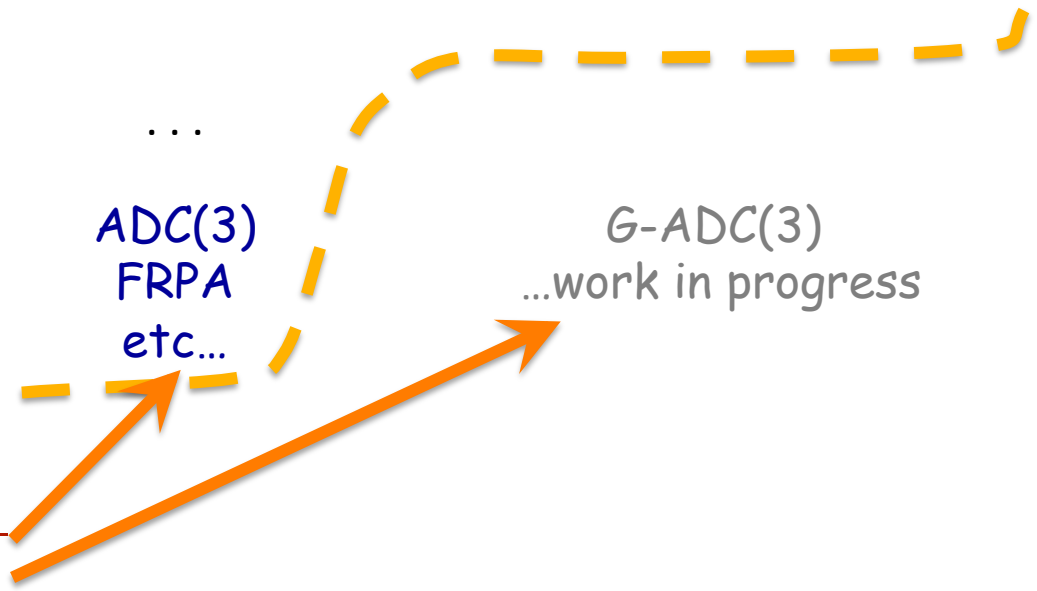

This is a ***non-perturbative all-orders resummation*** — NOT a PT truncation!

Approaches in GF theory

Truncation scheme:

Dyson formulation (closed shells)

Gorkov formulation (semi-/doubly-magic)

1st order: Hartree-Fock HF-Bogolioubov

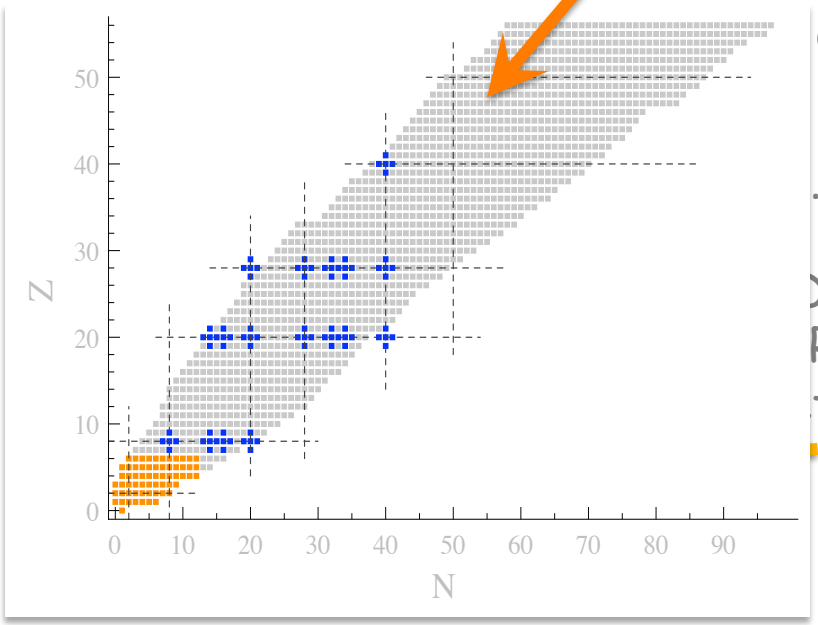

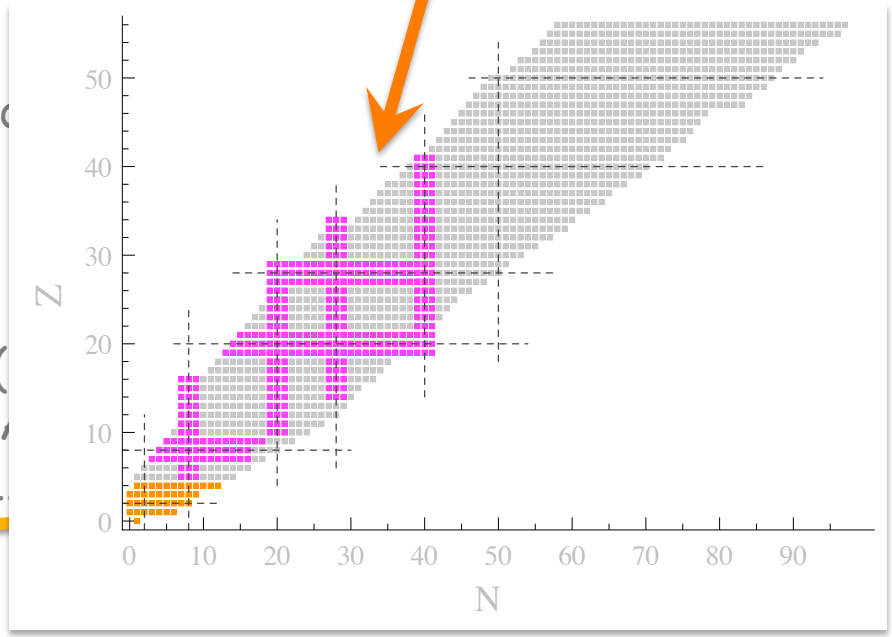

pics. credits: V. Somà

Inclusion of NNN forces

- Second order PT diagrams with 3BFs:

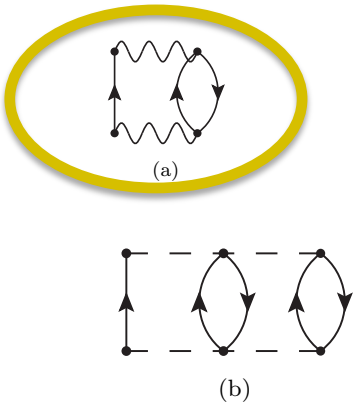

A. Carbone, CB, et al., Phys. Rev. C**88**, 054326 (2013) and F. Raimondi, CB, in preparation (2017).

- Third order PT diagrams with 3BFs:

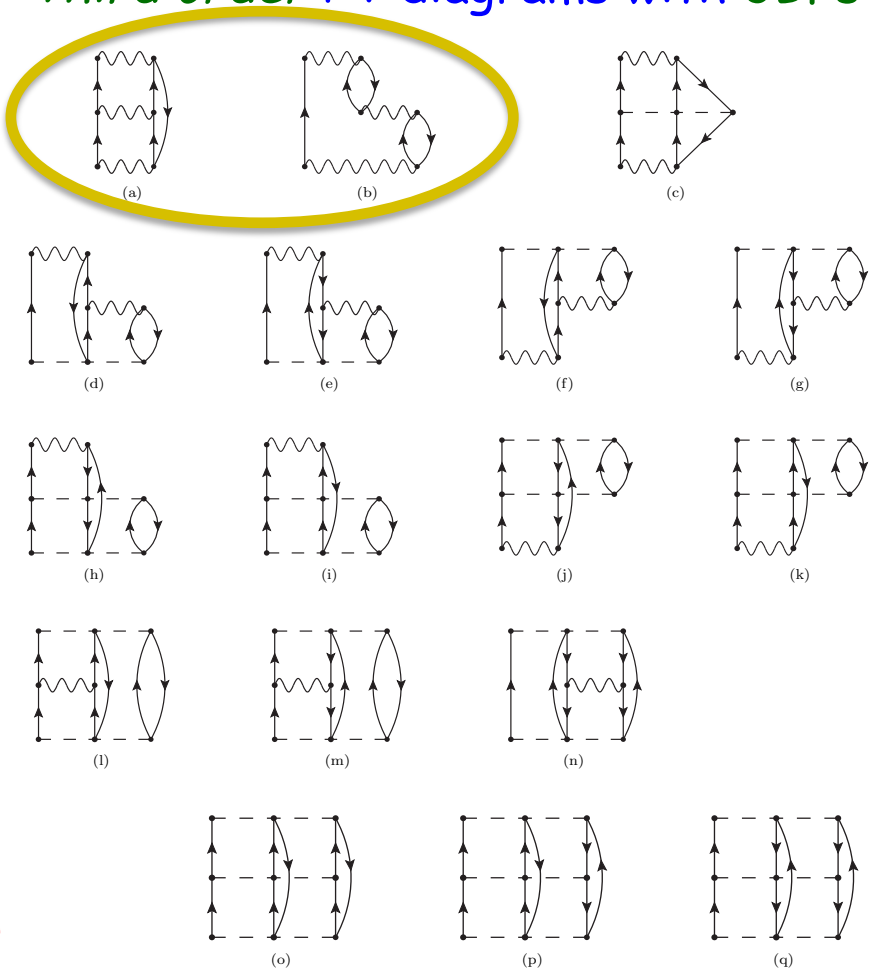

FIG. 5. 1PI, *skeleton* and *interaction irreducible* self-energy diagrams appearing at 3^{rd}-order in perturbative expansion (7), making use of the effective hamiltonian of Eq. (9).

➔ Use of irreducible 2-body interactions

➔ Need to correct the Koltun sum rule (for energy)

➔ 3p2h/3h2p terms relevant to next-generation high-precision methods.

Inclusion of NNN forces

- Second order PT diagrams with 3BFs:

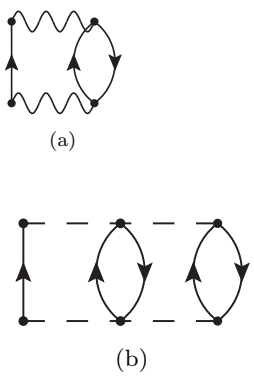

A. Carbone, CB, et al., Phys. Rev. C**88**, 054326 (2013) and F. Raimondi, CB, in preparation (2017).

- Third order PT diagrams with 3BFs:

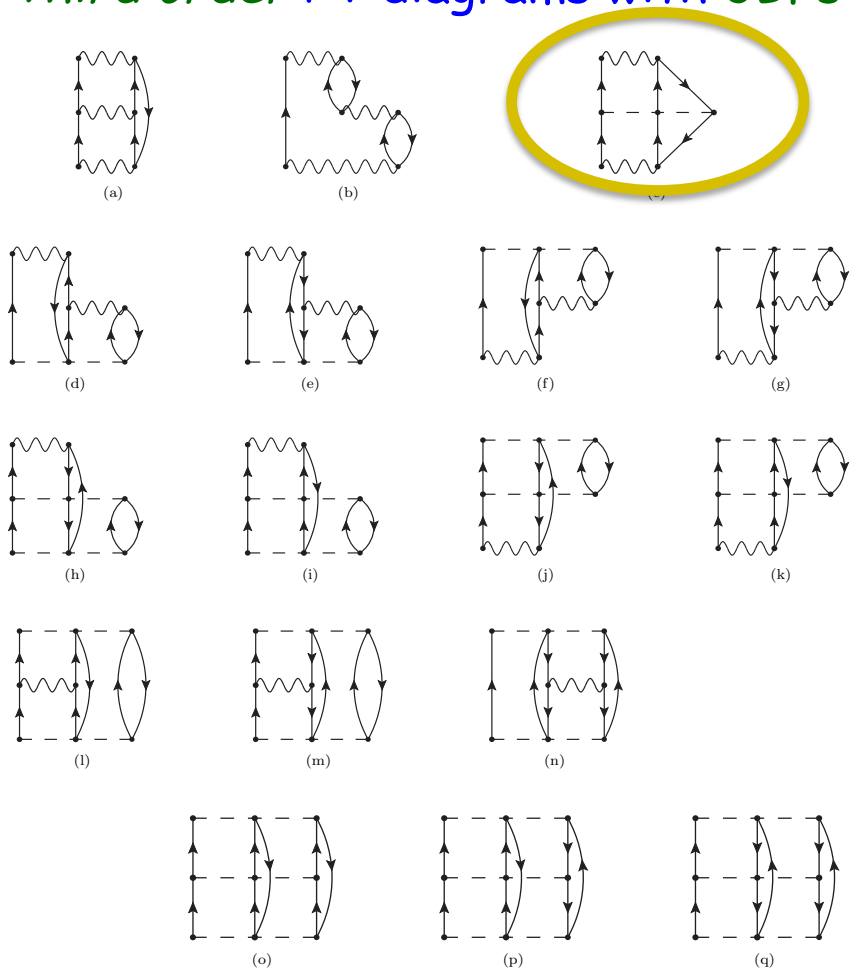

FIG. 5. 1PI, *skeleton* and *interaction irreducible* self-energy diagrams appearing at 3^{rd}-order in perturbative expansion (7), making use of the effective hamiltonian of Eq. (9).

➔ Use of irreducible 2-body interactions

➔ Need to correct the Koltun sum rule (for energy)

➔ 3p2h/3h2p terms relevant to next-generation high-precision methods.

Inclusion of NNN forces

First interactions irreducible 3NF term:

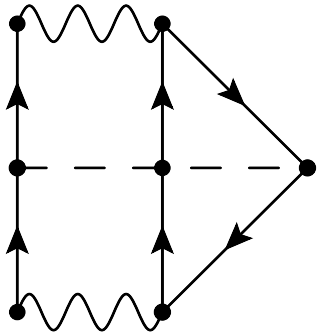

F. Raimondi, CB, arXiv:1701.08127v1 [nucl-th] and PhysRevC in preparation (2017).

while the one connecting through a hole-particle (hp) interaction gives

$$\begin{aligned}\mathbf{D}^{hp}_{(k_1k_2n_3),(k_4k_5n_6)} &= \frac{1}{2}\Big((\mathcal{Y}^{k_2}_{\mu}\mathcal{X}^{n_3}_{\rho})^{*}\,\widetilde{V}_{\mu\nu,\lambda\rho}\,\mathcal{Y}^{k_5}_{\lambda}\mathcal{X}^{n_6}_{\nu}\,\delta_{k_1k_4} \\ &- (\mathcal{Y}^{k_2}_{\mu}\mathcal{X}^{n_3}_{\rho})^{*}\,\widetilde{V}_{\mu\nu,\lambda\rho}\,\mathcal{Y}^{k_4}_{\lambda}\mathcal{X}^{n_6}_{\nu}\,\delta_{k_1k_5} \\ &- (\mathcal{Y}^{k_1}_{\mu}\mathcal{X}^{n_3}_{\rho})^{*}\,\widetilde{V}_{\mu\nu,\lambda\rho}\,\mathcal{Y}^{k_5}_{\lambda}\mathcal{X}^{n_6}_{\nu}\,\delta_{k_2k_4} \\ &+ (\mathcal{Y}^{k_1}_{\mu}\mathcal{X}^{n_3}_{\rho})^{*}\,\widetilde{V}_{\mu\nu,\lambda\rho}\,\mathcal{Y}^{k_4}_{\lambda}\mathcal{X}^{n_6}_{\nu}\,\delta_{k_2k_5}\Big)\end{aligned}$$

We now turn to the Feynman diagram of Fig. 3c, which is the focus work. To our knowledge the ADC formulas arising from this term presented before. The Feynman rules give the following expression for

$$\Sigma^{(3c)}_{\alpha\beta}(\omega) = -\frac{(\hbar)^4}{4}\int\frac{\mathrm{d}\omega_1}{2\pi\mathrm{i}}\int\frac{\mathrm{d}\omega_2}{2\pi\mathrm{i}}\int\frac{\mathrm{d}\omega_3}{2\pi\mathrm{i}}\int\frac{\mathrm{d}\omega_4}{2\pi\mathrm{i}}\sum_{\substack{\gamma\delta\nu\mu\epsilon\lambda\\ \xi\eta\theta\sigma\tau\chi}}\widetilde{V}_{\alpha\gamma,\delta\nu}\; g_{\xi\gamma}(\omega_3)\; g_{\nu\lambda}$$

$$g_{\delta\epsilon}(\omega_1)\; W_{\mu\epsilon\lambda,\xi\eta\theta}\; g_{\theta\tau}(\omega-\omega_2+\omega_4)\; g_{\eta\sigma}(\omega_2)\; g_{\chi\mu}(\omega_4)\; \widetilde{V}_{\sigma\tau,}$$

By performing the four integrals in the complex plane, we find six term ing to the different time orderings of the three interactions. Altogether

$$\Sigma^{(3c)}_{\alpha\beta}(\omega) = \frac{1}{4}\sum_{\substack{\gamma\delta\nu\mu\epsilon\lambda\\ \xi\eta\theta\sigma\tau\chi}}\widetilde{V}_{\alpha\gamma,\delta\nu}W_{\epsilon\lambda\mu,\eta\theta\xi}\widetilde{V}_{\sigma\tau,\beta\chi}\times$$

$$\Bigg(-\sum_{\substack{n_1n_2k_3\\ n_4n_5k_6}}\frac{(\mathcal{X}^{n_1}_{\delta}\mathcal{X}^{n_2}_{\nu}\mathcal{Y}^{k_3}_{\gamma})^{*}\mathcal{X}^{n_1}_{\epsilon}\mathcal{X}^{n_2}_{\lambda}\mathcal{Y}^{k_3}_{\xi}(\mathcal{X}^{n_4}_{\eta}\mathcal{X}^{n_5}_{\theta}\mathcal{Y}^{k_6}_{\mu})^{*}\mathcal{X}^{n_4}_{\sigma}\mathcal{X}^{n}_{\tau}}{(\hbar\omega-(\varepsilon^{+}_{n_1}+\varepsilon^{+}_{n_2}-\varepsilon^{-}_{k_3})+\mathrm{i}\eta)\,(\hbar\omega-(\varepsilon^{+}_{n_4}+\varepsilon^{+}_{n_5}-\varepsilon^{-}_{k}}$$

$$+\sum_{\substack{k_1k_2n_3\\ n_4n_5k_6}}\frac{\mathcal{Y}^{k_1}_{\delta}\mathcal{Y}^{k_2}_{\nu}\mathcal{X}^{n_3}_{\gamma}(\mathcal{Y}^{k_1}_{\epsilon}\mathcal{Y}^{k_2}_{\lambda}\mathcal{Y}^{k_6}_{\mu}\mathcal{X}^{n_4}_{\eta}\mathcal{X}^{n_5}_{\theta}\mathcal{X}^{n_3}_{\xi})^{*}\mathcal{X}^{n_4}_{\sigma}\mathcal{X}^{n_5}_{\tau}}{(\varepsilon^{-}_{k_1}+\varepsilon^{-}_{k_2}+\varepsilon^{-}_{k_6}-\varepsilon^{+}_{n_3}-\varepsilon^{+}_{n_4}-\varepsilon^{+}_{n_5})\,(\hbar\omega-(\varepsilon^{+}_{n_4}+\varepsilon^{+}_{n_5}$$

$$+\sum_{\substack{k_1k_2n_3\\ n_4n_5k_6}}\frac{(\mathcal{X}^{n_4}_{\delta}\mathcal{X}^{n_5}_{\nu}\mathcal{Y}^{k_6}_{\gamma})^{*}\mathcal{X}^{n_4}_{\epsilon}\mathcal{X}^{n_5}_{\lambda}\mathcal{X}^{n_3}_{\mu}\mathcal{Y}^{k_1}_{\eta}\mathcal{Y}^{k_2}_{\theta}\mathcal{Y}^{k_6}_{\xi}(\mathcal{Y}^{k_1}_{\sigma}\mathcal{Y}^{k_2}_{\tau}}{(\hbar\omega-(\varepsilon^{+}_{n_4}+\varepsilon^{+}_{n_5}-\varepsilon^{-}_{k_6})+\mathrm{i}\eta)\,(\varepsilon^{-}_{k_1}+\varepsilon^{-}_{k_2}+\varepsilon^{-}_{k_6}-\varepsilon^{+}_{n_3}-$$

$$-\sum_{\substack{k_1k_2n_3\\ k_4k_5n_6}}\frac{\mathcal{Y}^{k_1}_{\delta}\mathcal{Y}^{k_2}_{\nu}\mathcal{X}^{n_3}_{\gamma}(\mathcal{Y}^{k_1}_{\epsilon}\mathcal{Y}^{k_2}_{\lambda}\mathcal{X}^{n_3}_{\xi})^{*}\mathcal{Y}^{k_4}_{\eta}\mathcal{Y}^{k_5}_{\theta}\mathcal{X}^{n_6}_{\mu}(\mathcal{Y}^{k_4}_{\sigma}\mathcal{Y}^{k_5}_{\tau}\mathcal{X}^{n_6}_{\chi}}{(\hbar\omega-(\varepsilon^{-}_{k_1}+\varepsilon^{-}_{k_2}-\varepsilon^{+}_{n_3})-\mathrm{i}\eta)\,(\hbar\omega-(\varepsilon^{-}_{k_4}+\varepsilon^{-}_{k_5}-\varepsilon^{+}_{n_6})}$$

$$-\sum_{\substack{k_1k_2n_3\\ n_4n_5k_6}}\frac{\mathcal{Y}^{k_1}_{\delta}\mathcal{Y}^{k_2}_{\nu}\mathcal{X}^{n_3}_{\gamma}(\mathcal{Y}^{k_1}_{\epsilon}\mathcal{Y}^{k_2}_{\lambda}\mathcal{Y}^{k_6}_{\mu}\mathcal{X}^{n_4}_{\eta}\mathcal{X}^{n_5}_{\theta}\mathcal{X}^{n_3}_{\xi})^{*}\mathcal{X}^{n_4}_{\sigma}\mathcal{X}^{n_5}_{\tau}}{(\hbar\omega-(\varepsilon^{-}_{k_1}+\varepsilon^{-}_{k_2}+\varepsilon^{-}_{k_6}-\varepsilon^{+}_{n_3})-\mathrm{i}\eta)\,(\varepsilon^{-}_{k_1}+\varepsilon^{-}_{k_2}+\varepsilon^{-}_{k_6}-\varepsilon^{+}_{n_3}-$$

$$-\sum_{\substack{k_1k_2n_3\\ n_4n_5k_6}}\frac{(\mathcal{X}^{n_4}_{\delta}\mathcal{X}^{n_5}_{\nu}\mathcal{Y}^{k_6}_{\gamma})^{*}\mathcal{X}^{n_4}_{\epsilon}\mathcal{X}^{n_5}_{\lambda}\mathcal{X}^{n_3}_{\mu}\mathcal{Y}^{k_1}_{\eta}\mathcal{Y}^{k_2}_{\theta}\mathcal{Y}^{k_6}_{\xi}(\mathcal{Y}^{k_1}_{\sigma}\mathcal{Y}^{k_2}_{\tau}}{(\varepsilon^{-}_{k_1}+\varepsilon^{-}_{k_2}+\varepsilon^{-}_{k_6}-\varepsilon^{+}_{n_3}-\varepsilon^{+}_{n_4}-\varepsilon^{+}_{n_5})\,(\hbar\omega-(\varepsilon^{-}_{k_1}+\varepsilon^{-}_{k_2}-$$

where the first (last) three terms correspond to forward-in-time (back Goldstone diagrams.

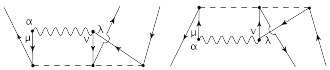

Figure 5: Diagrams of the ADC(3) coupling matrices with one effective 2NF $\widetilde{V}$ and one interaction-irreducible 3NF $\widetilde{W}$. The coupling matrix (a) is linked to $2p1h$ ISCs and corresponds to Eq. (45), while (b) is linked to $2h1p$ ISCs and corresponds to Eq. (46).

By comparing to the third order terms in Eq. (24), one see that the new contributions to the coupling matrices contain one effective 2NF and one interaction-irreducible 3NF. The following forward-in-time matrix can be singled out from either the second or third line of Eq. (44),

$$\mathbf{M}^{(2\mathrm{N}\ 3\mathrm{N}\ \mathrm{a})}_{(n_1n_2k_3)\alpha} \equiv \frac{1}{2\sqrt{2}}\,\frac{\mathcal{X}^{n_4}_{\xi}\mathcal{X}^{n_1}_{\rho}\mathcal{X}^{n_2}_{\sigma}\;W_{\xi\rho\sigma,\zeta\eta\theta}\;\mathcal{Y}^{k_3}_{\zeta}\mathcal{Y}^{k_5}_{\eta}\mathcal{Y}^{k_6}_{\theta}}{\varepsilon^{-}_{k_3}+\varepsilon^{-}_{k_5}+\varepsilon^{-}_{k_6}-\varepsilon^{+}_{n_1}-\varepsilon^{+}_{n_2}-\varepsilon^{+}_{n_4}}\;(\mathcal{Y}^{k_5}_{\mu}\mathcal{Y}^{k_6}_{\nu}\mathcal{X}^{n_4}_{\lambda})^{*}\;\widetilde{V}_{\mu\nu,\alpha\lambda}\;, \quad (45)$$

while in the last two lines of Eq. (44) we read the backward-in-time coupling matrix:

$$\mathbf{N}^{(2\mathrm{N}\ 3\mathrm{N}\ \mathrm{a})}_{\alpha(k_1k_2n_3)} \equiv -\frac{1}{2\sqrt{2}}\,\widetilde{V}_{\alpha\lambda,\mu\nu}\;(\mathcal{Y}^{k_4}_{\lambda}\mathcal{X}^{n_5}_{\mu}\mathcal{X}^{n_6}_{\nu})^{*}\frac{\mathcal{X}^{n_3}_{\rho}\mathcal{X}^{n_5}_{\sigma}\mathcal{X}^{n_6}_{\xi}\;W_{\rho\sigma\xi,\theta\zeta\eta}\;\mathcal{Y}^{k_4}_{\theta}\mathcal{Y}^{k_1}_{\zeta}\mathcal{Y}^{k_2}_{\eta}}{\varepsilon^{-}_{k_1}+\varepsilon^{-}_{k_2}+\varepsilon^{-}_{k_4}-\varepsilon^{+}_{n_3}-\varepsilon^{+}_{n_5}-\varepsilon^{+}_{n_6}}\;. \quad (46)$$

The diagrammatic representations of Eqs. (45) and (46) are displayed in Fig. 5.

The only interaction matrix that connects $2p1h$ ISCs through a 3NF is found from the first term of Eq. (44),

$$\mathbf{C}^{3N}_{(n_1n_2k_3),(n_4n_5k_6)} \equiv -\frac{1}{2}\mathcal{X}^{n_1}_{\nu}\mathcal{X}^{n_2}_{\mu}\mathcal{Y}^{k_3}_{\rho}\;W_{\nu\mu\lambda,\epsilon\eta\rho}\;(\mathcal{X}^{n_4}_{\epsilon}\mathcal{X}^{n_5}_{\eta}\mathcal{Y}^{k_6}_{\lambda})^{*}\;, \quad (47)$$

which is explicitly antisymmetric in the particle indexes. With Eqs. (47) and (27) we can rewrite the first term of Eq. (44) as,

$$\mathbf{M}^{\dagger(\mathrm{I\text{-}2N})}_{\alpha r}\,\frac{1}{\hbar\omega-E_r}\,\mathbf{C}^{3N}_{rr'}\,\frac{1}{\hbar\omega-E_{r'}}\,\mathbf{M}^{(\mathrm{I\text{-}2N})}_{r'\beta}\;. \quad (48)$$

The expression (48) contains only the first order contribution in the interaction matrix expansion, corresponding to the second term in the r.h.s. of Eq. (23), for $B=\mathbf{C}^{3N}$. This is resummed to all order by diagonalizing the Dyson matrix (19), which will automatically include *all* the higher order terms in the expansion.

From the fourth term of Eq. (44), we single out the only backward-in-time interaction matrix connecting two $2h1p$ configurations through a 3N interaction, that is

$$\mathbf{D}^{3N}_{(k_1k_2n_3),(k_4k_5n_6)} \equiv -\frac{1}{2}(\mathcal{Y}^{k_1}_{\nu}\mathcal{Y}^{k_2}_{\mu}\mathcal{X}^{n_3}_{\rho})^{*}\;W_{\nu\mu\lambda,\epsilon\eta\rho}\;\mathcal{Y}^{k_4}_{\epsilon}\mathcal{Y}^{k_5}_{\eta}\mathcal{X}^{n_6}_{\lambda}\;, \quad (49)$$

which is also explicitly antisymmetric in the hole indexes. With Eqs. (49) and (28) we associate the fourth term of Eq. (44) to

$$\mathbf{N}^{(\mathrm{I\text{-}2N})}_{\alpha s}\,\frac{1}{\hbar\omega-E_s}\,\mathbf{D}^{3N}_{ss'}\,\frac{1}{\hbar\omega-E_{s'}}\,\mathbf{N}^{\dagger(\mathrm{I\text{-}2N})}_{s'\beta}\;. \quad (50)$$

UNIVERSITY OF SURREY

Ab-initio Nuclear Computation & BcDor code

BoccaDorata code:
(*C. Barbieri* 2006-16
V. Somà 2010-15
A. Cipollone 2011-14)

- Provides a *C++ class library* for handling many-body propagators (≈40,000 lines, MPI&OpenMP based).
- Allows to solve for nuclear spectral functions, many-body propagators, RPA responses, coupled cluster equations and effective interaction/charges for the shell model.

Code history:

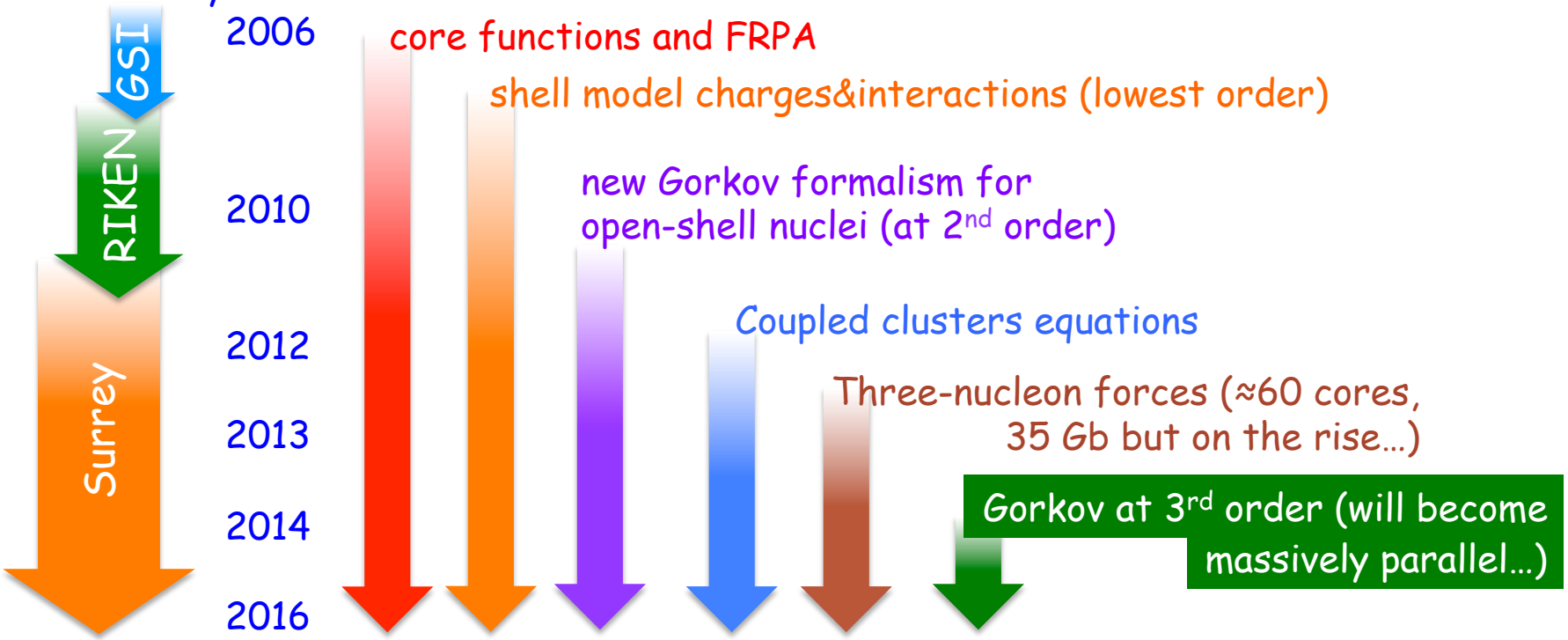

… applications …

Ab-initio Nuclear Computation & BcDor code

http://personal.ph.surrey.ac.uk/~cb0023/bcdor/

Computational Many-Body Physics

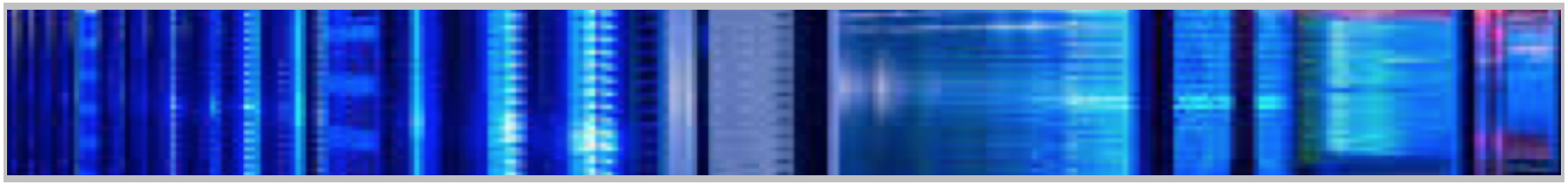

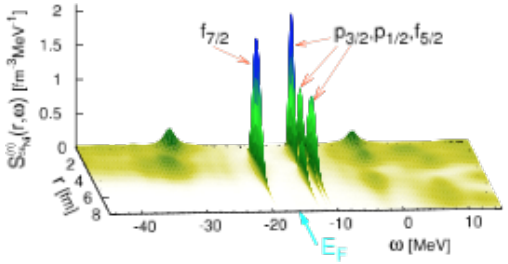

Download

Documentation

Welcome

From here you can download a public version of my self-consistent Green's function (SCGF) code for nuclear physics. This is a code in J-coupled scheme that allows the calculation of the single particle propagators (a.k.a. one-body Green's functions) and other many-body properties of spherical nuclei.

This version allows to:

- Perform Hartree-Fock calculations.
- Calculate the the correlation energy at second order in perturbation theory (MBPT2).
- Solve the Dyson equation for propagators (self consistently) up to second order in the self-energy.
- Solve coupled cluster CCD (doubles only!) equations.

When using this code you are kindly invited to follow the creative commons license agreement, as detailed at the weblinks below. In particular, we kindly ask you to refer to the publications that led the development of this software.

Relevant references (which can also help in using this code) are:

Prog. Part. Nucl. Phys. 52, p. 377 (2004),
Phys. Rev. A76, 052503 (2007),
Phys. Rev. C79, 064313 (2009),
Phys. Rev. C89, 024323 (2014)

Results for the N-O-F chains

A. Cipollone, CB, P. Navrátil, Phys. Rev. Lett. **111**, 062501 (2013)
and Phys. Rev. C **92**, 014306 (2015)

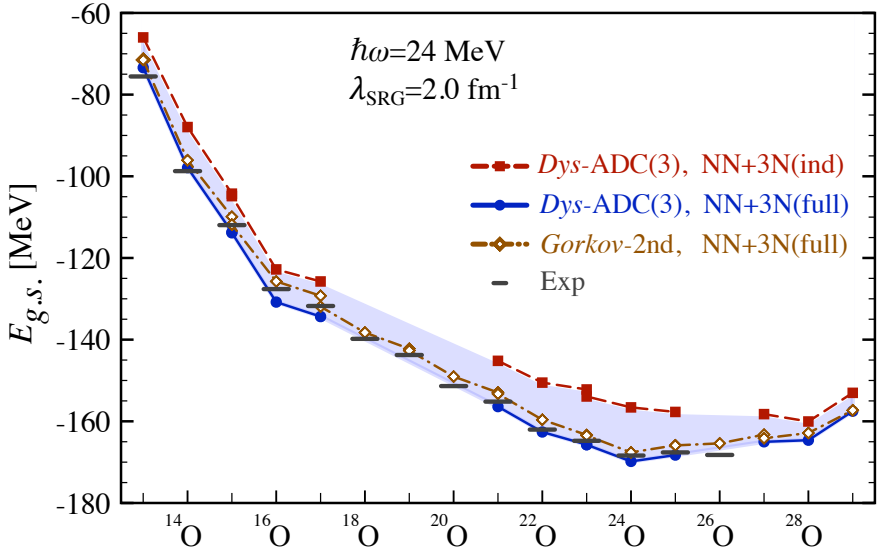

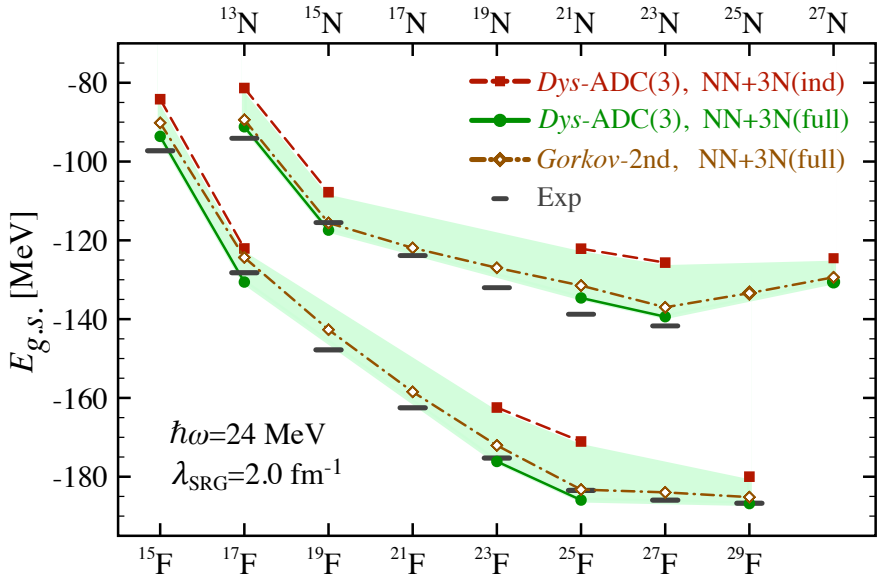

→ 3NF crucial for reproducing binding energies and driplines around oxygen

→ cf. microscopic shell model [Otsuka et al, PRL**105**, 032501 (2010).]

UNIVERSITY OF SURREY

N3LO (Λ = 500Mev/c) chiral NN interaction evolved to 2N + 3N forces (2.0fm^{-1})
N2LO (Λ = 400Mev/c) chiral 3N interaction evolved (2.0fm^{-1})

Neighbouring Ar, K, Ca, Sc, and Ti chains

V. Somà, CB *et al.* Phys. Rev. C**89**, 061301R (2014)

Two-neutron separation energies predicted by chiral NN[EM(500)]+3NF[N2LO(400)]:

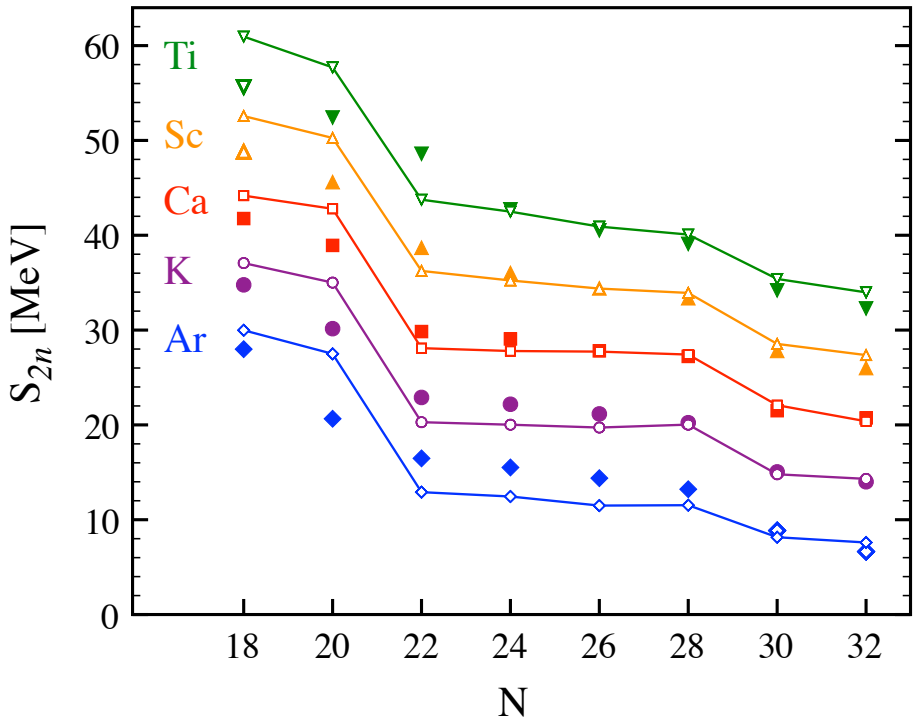

→ First *ab-initio* calculation over a contiguous portion of the nuclear chart—open shells are now possible through the Gorkov-GF formalism

PRL 117, 052501 (2016) PHYSICAL REVIEW LETTERS week ending 29 JULY 2016

Radii and Binding Energies in Oxygen Isotopes: A Challenge for Nuclear Forces

V. Lapoux,[1,*] V. Somà,[1] C. Barbieri,[2] H. Hergert,[3] J. D. Holt,[4] and S. R. Stroberg[4]

- New fits of chiral interactions (NNLOsat) highly improve comparison to data

- Deficiencies remain for neutron rich isotopes

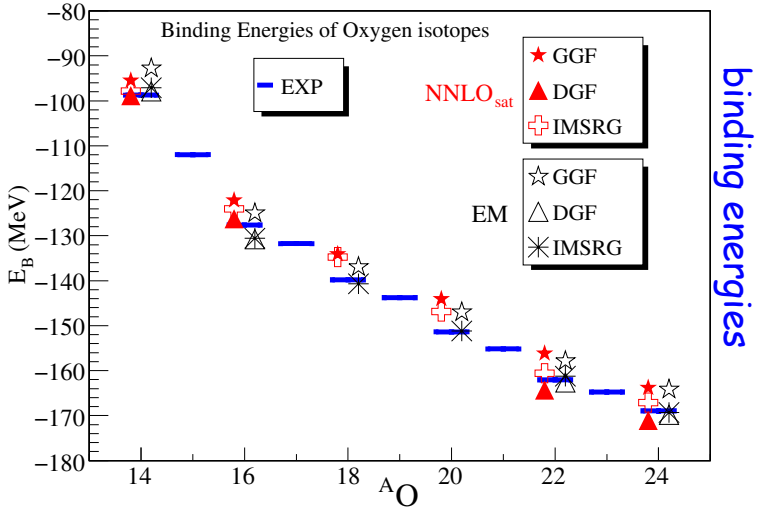

FIG. 1. Oxygen binding energies. Results from SCGF and IMSRG calculations performed with EM [20–22] and $NNLO_{sat}$ [26] interactions are displayed along with available experimental data.

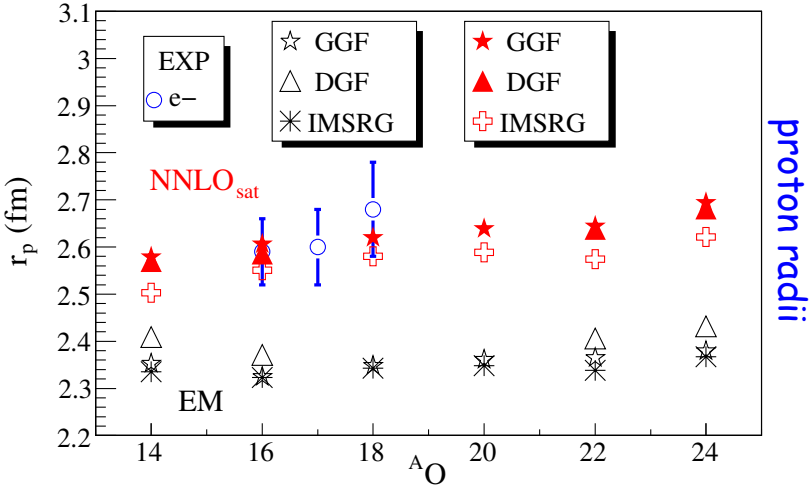

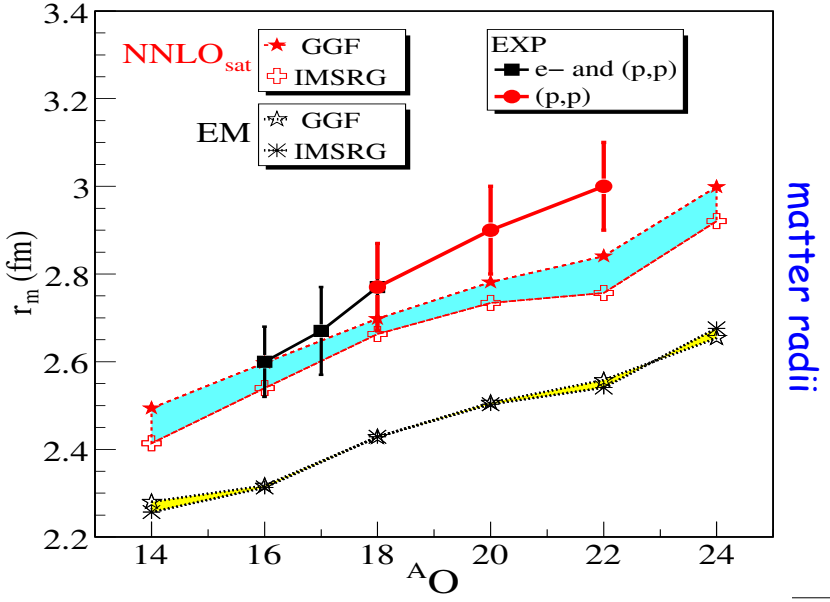

charge radii in the pf shell

Size of radii not prefect but remains overall correct throughout the ***pf*** shell with NNLO-sat.

This suggests that saturation is indeed under control.

➔ Improvements of many-body truncations beyond 2nd order Gorkov will also be relevant.

(work in progress!)

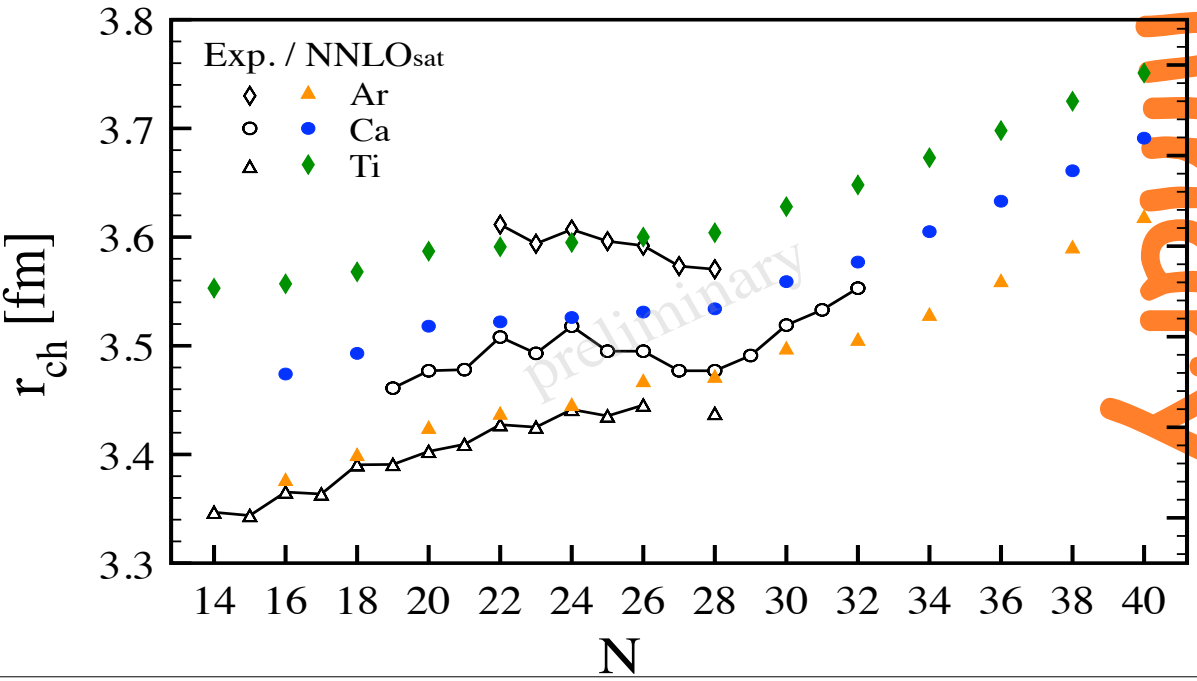

Preliminary

Bubble nuclei... ^{34}Si prediction

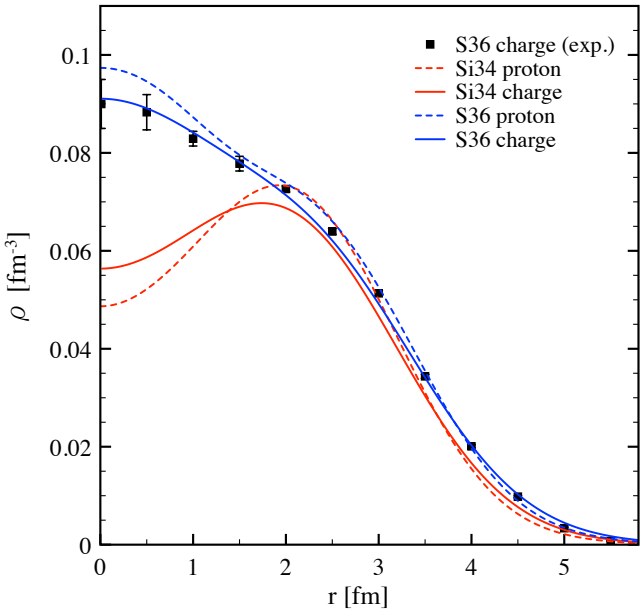

Duguet, Somà, CB, et al. arXiv:1611.08570 [nucl-th]

- ^{34}Si is unstable, charge distribution still unknown

- Suggested central depletion from mean-field simulations

- *Ab-initio* theory confirms predictions

Validated by charge distributions and neutron quasiparticle spectra:

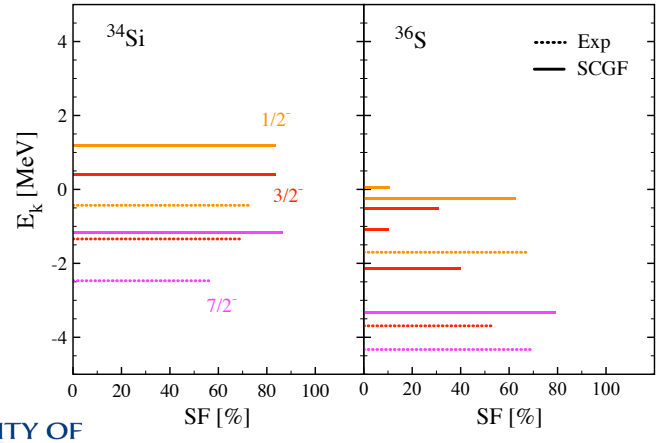

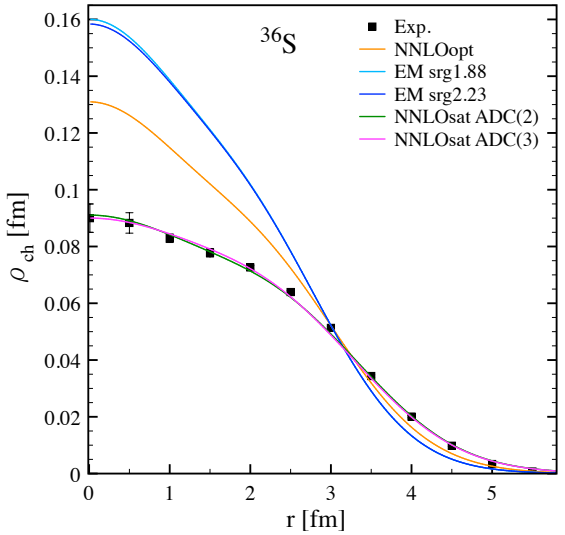

UNIVERSITY OF SURREY

Proton spectral strength in Oxygen

A. Cipollone, CB, P. Navrátil, Phys. Rev. Lett. **111**, 062501 (2013)
and Phys. Rev. C **92**, 014306 (2015)
and ***in preparation***

More in detail:

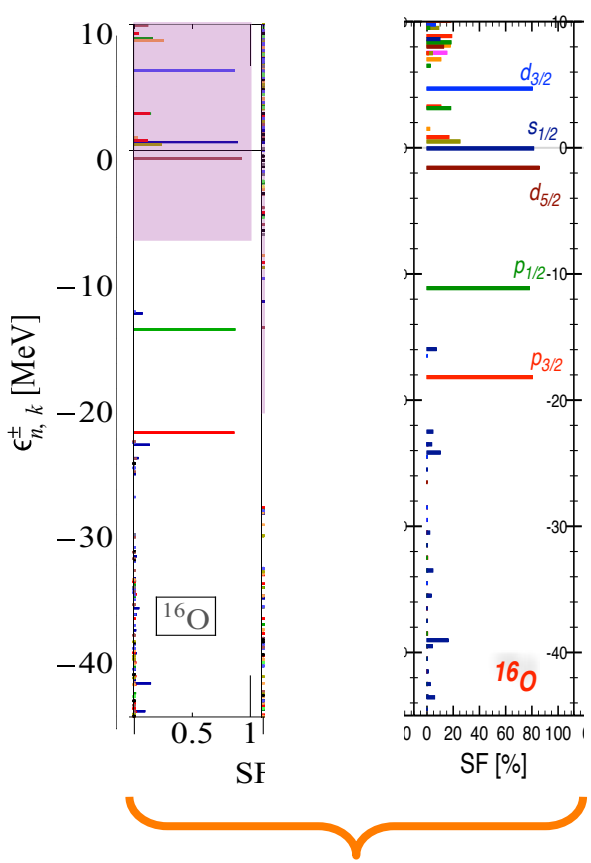

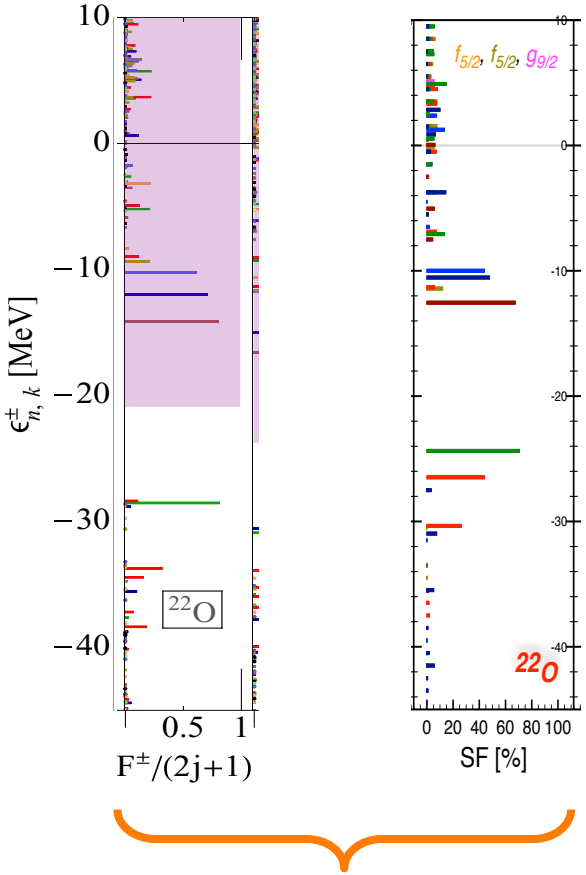

Quenching of absolute spectroscopic factors

[CB, *Phys. Rev. Lett.* **103**, 202520 (2009)]

Overall quenching of *spectroscopic factors* is driven by:

SRC → *~10%*

part-vibr. coupling → *dominant*

"shell-model" → *in open shell*

…with analogous conclusions for ^{48}Ca

		10 osc. shells			Exp. [30]	$1p0f$ space		
		FRPA (SRC)	full FRPA	FRPA $+\Delta Z_\alpha$		FRPA	SM	ΔZ_α
	^{57}Ni:							
^{57}Ni	$\nu 1p_{1/2}$	0.96	0.63	0.61		0.79	0.77	-0.02
	$\nu 0f_{5/2}$	0.95	0.59	0.55		0.79	0.75	-0.04
	$\nu 1p_{3/2}$	0.95	0.65	0.62	0.58(11)	0.82	0.79	-0.03
^{55}Ni	^{55}Ni:							
	$\nu 0f_{7/2}$	0.95	0.72	0.69		0.89	0.86	-0.03
		①	② + ③			③		

$$Z_\alpha = \int d^3r\, |\psi_\alpha^{overlap}(\mathbf{r})|^2 = \left. \frac{1}{1 - \frac{\partial \Sigma_{\hat{\alpha}\hat{\alpha}}(\omega)}{\partial \omega}} \right|_{\omega=\varepsilon_\alpha}$$

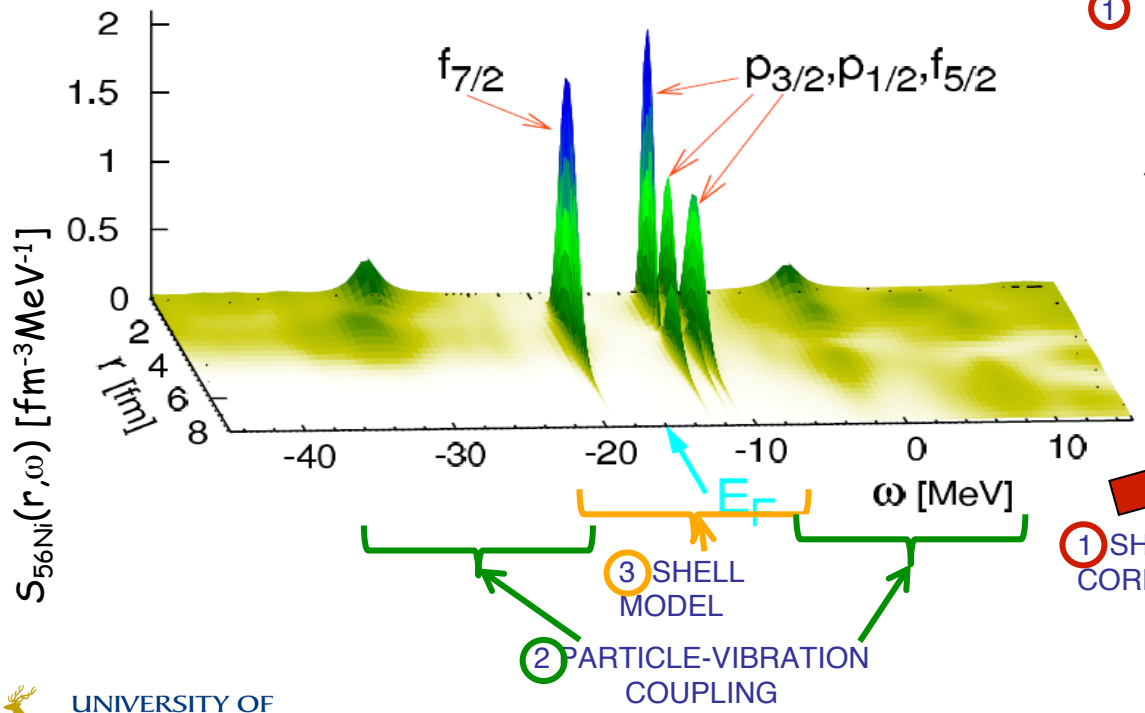

Z/N asymmetry dependence of SFs - Theory

Ab-initio calculations explain (a very weak) the Z/N dependence but the effect is much lower than suggested by direct knockout

Rather the quenching is high correlated to the gap at the Femi surface.

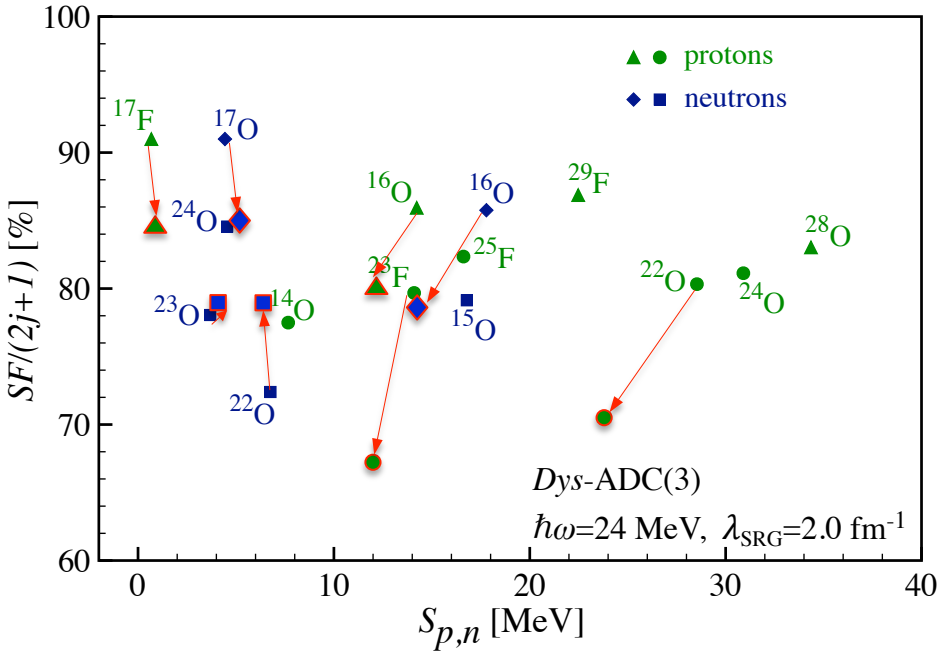

A. Cipollone, CB, P Navrátil
Phys. Rev. C**92**, 014306 (2015)

Spectroscopic factor are strongly correlated to p-h gaps:

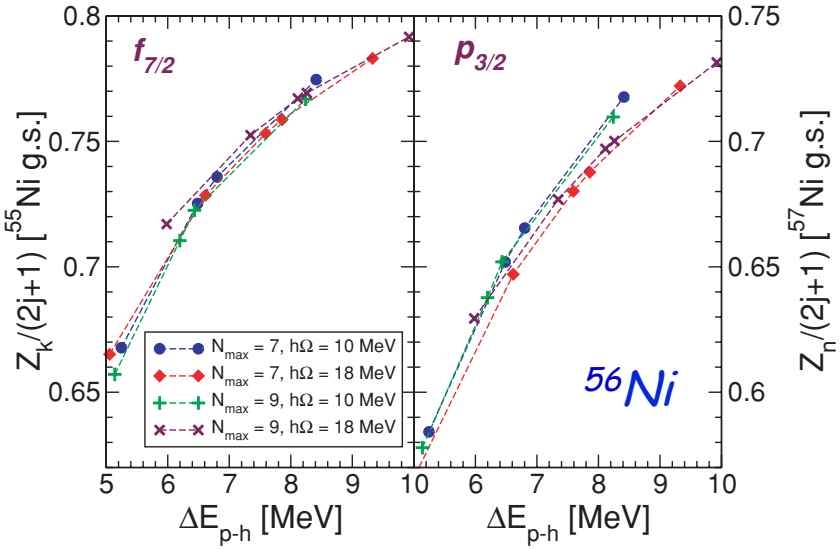

CB, M. Hjorth-Jensen,
Phys. Rev. C **79**, 064313 (2009)

Z/N asymmetry dependence of SFs - Theory

Ab-initio calculations explain (a very weak) the Z/N dependence but the effect is much lower than suggested by direct knockout

Rather the quenching is high correlated to the gap at the Femi surface.

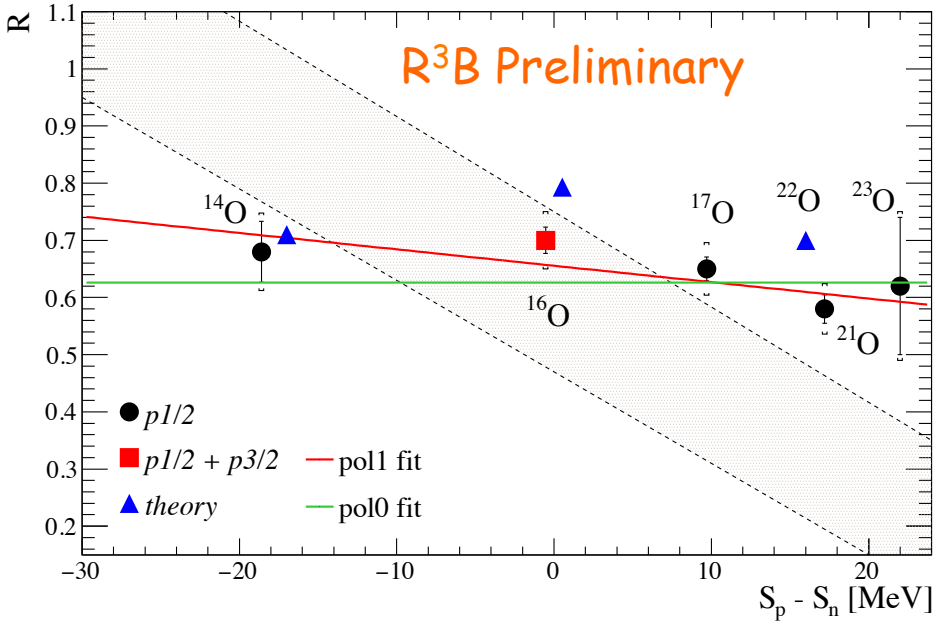

Spectroscopic factor are strongly correlated to p-h gaps:

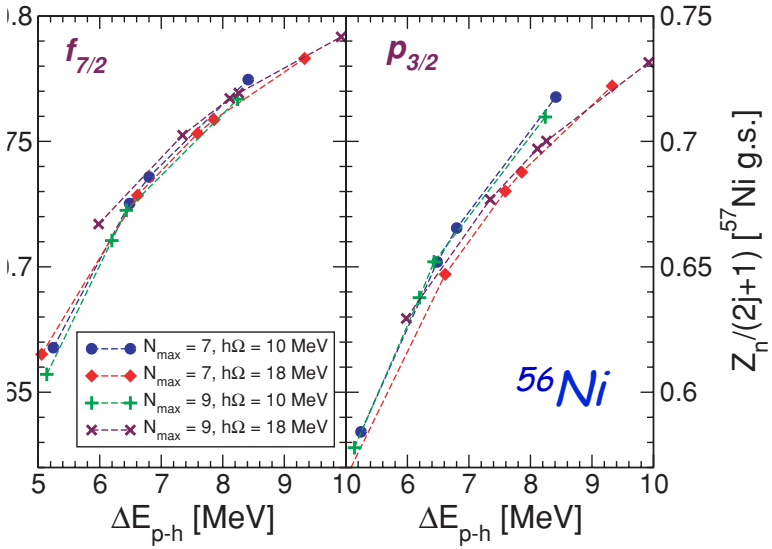

A. Cipollone, CB, P Navrátil
Phys. Rev. C**92**, 014306 (2015)

CB, M. Hjorth-Jensen,
Phys. Rev. C **79**, 064313 (2009)

Local vs. non-local chiral N^{2}LO NNN interaction — by P. Navrátil

- Local: chiral N^{3}LO NN+ N^{2}LO 3N500
  - c_D=-0.2 c_E=-0.205 (^{3}H E_{gs}=-8.48 MeV)
  - ^{4}He

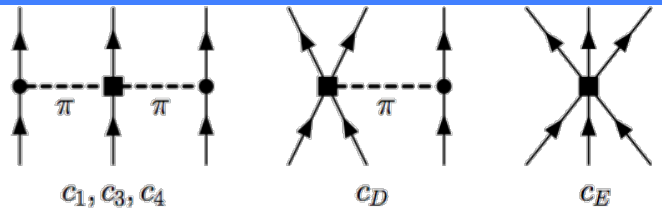

<H>=-28.4939 <V3b_2pi>= -5.8819 <V3b_D>= -0.2206 <V3b_E>= 1.2665

- Non-local: chiral N^{2}LO$_{sat}$ NN+3N
  - c_D=+0.8168 c_E=-0.0396 (^{3}H E_{gs}=-8.53 MeV)
  - ^{4}He

<H>=-28.4596 <V3b_2pi>= -4.7260 <V3b_D>= 1.3897 <V3b_E>= 0.4174

- Local/Non-local: chiral N^{3}LO NN+ N^{2}LO

$$F(\tfrac{1}{2}(\pi_1^2+\pi_2^2);\Lambda_{\text{nonloc}})\, W_1^Q(\Lambda_{\text{loc}})\, F(\tfrac{1}{2}(\pi_1^2+\pi_2^2);\Lambda_{\text{nonloc}})$$

Use completeness in HO basis to calculate products of *F W F*

  - c_D=+0.7 c_E=-0.06 (^{3}H E_{gs}=-8.44 MeV)
  - ^{4}He

<H>=-28.2530 <V3b_2pi>= -4.8124 <V3b_D>= 0.7414 <V3b_E>= 0.4255

N3LO(500) + nln 3NF

SCGF – Gorkov-ADC(2)

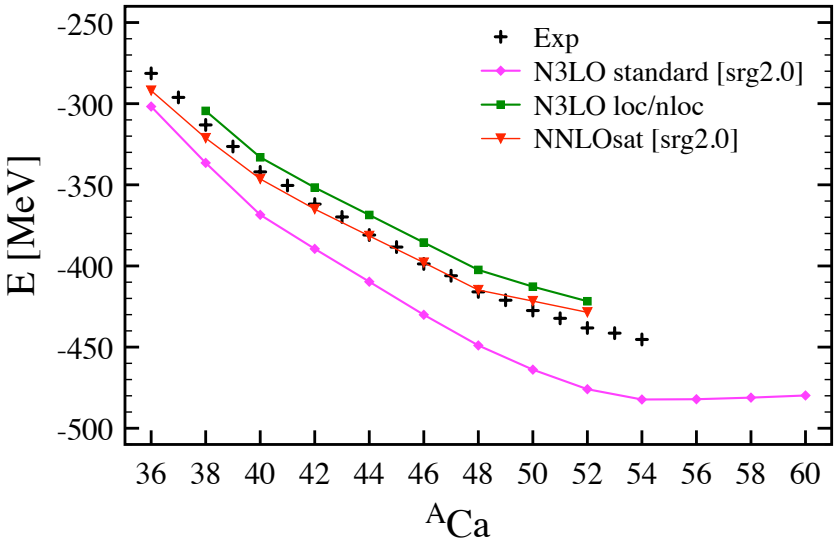

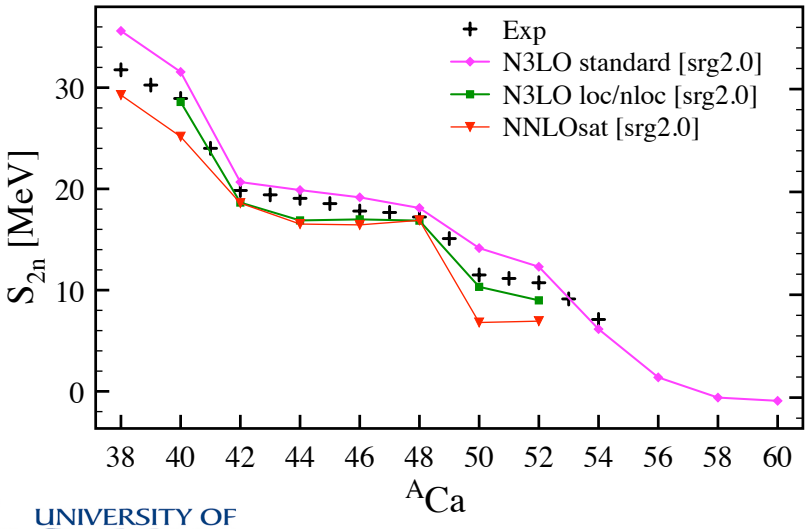

PRELIMINARY

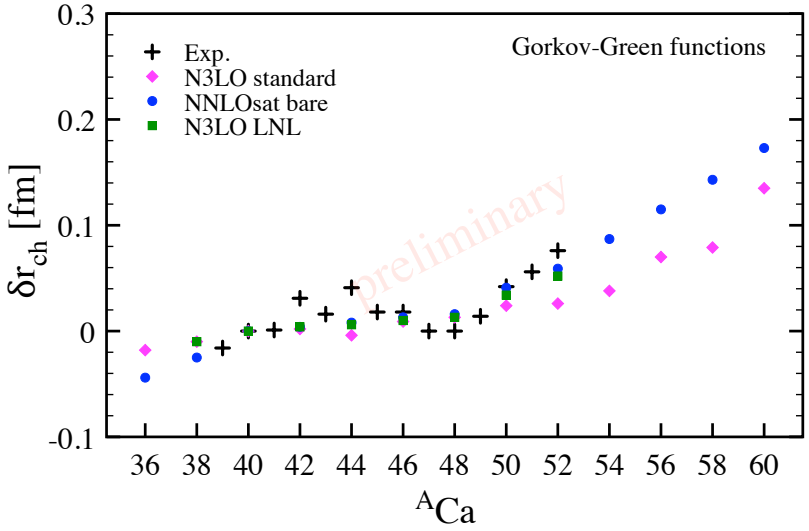

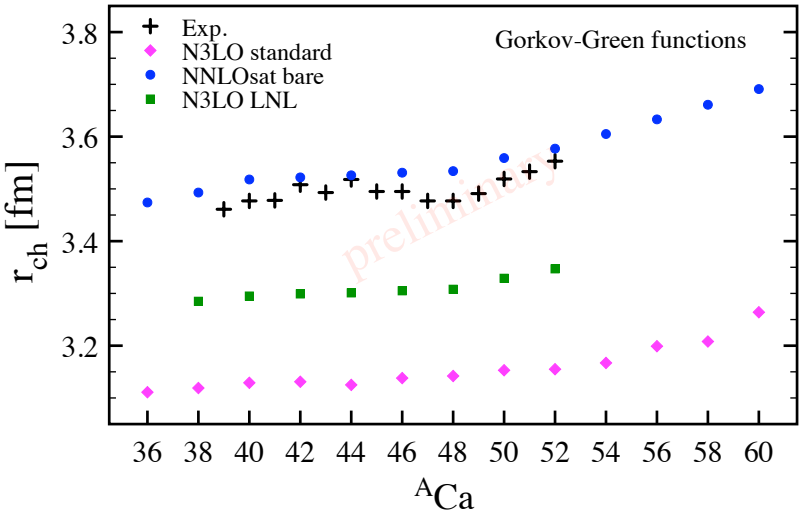

UNIVERSITY OF SURREY

Study of nuclear interactions from Lattice QCD

In collaboration with:

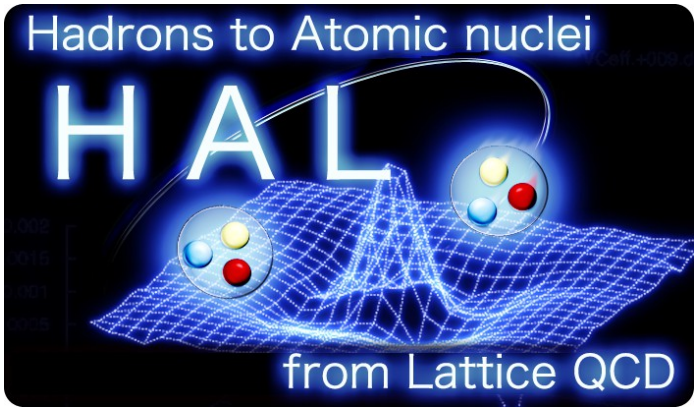

Approaches to nuclei from LQCD

$$L = -\frac{1}{4} G^{a}_{\mu\nu} G^{\mu\nu}_{a} + \bar{q}\,\gamma^{\mu}\left(i\partial_{\mu} - g\,t^{a}\,A^{a}_{\mu}\right)q - m\,\bar{q}\,q$$

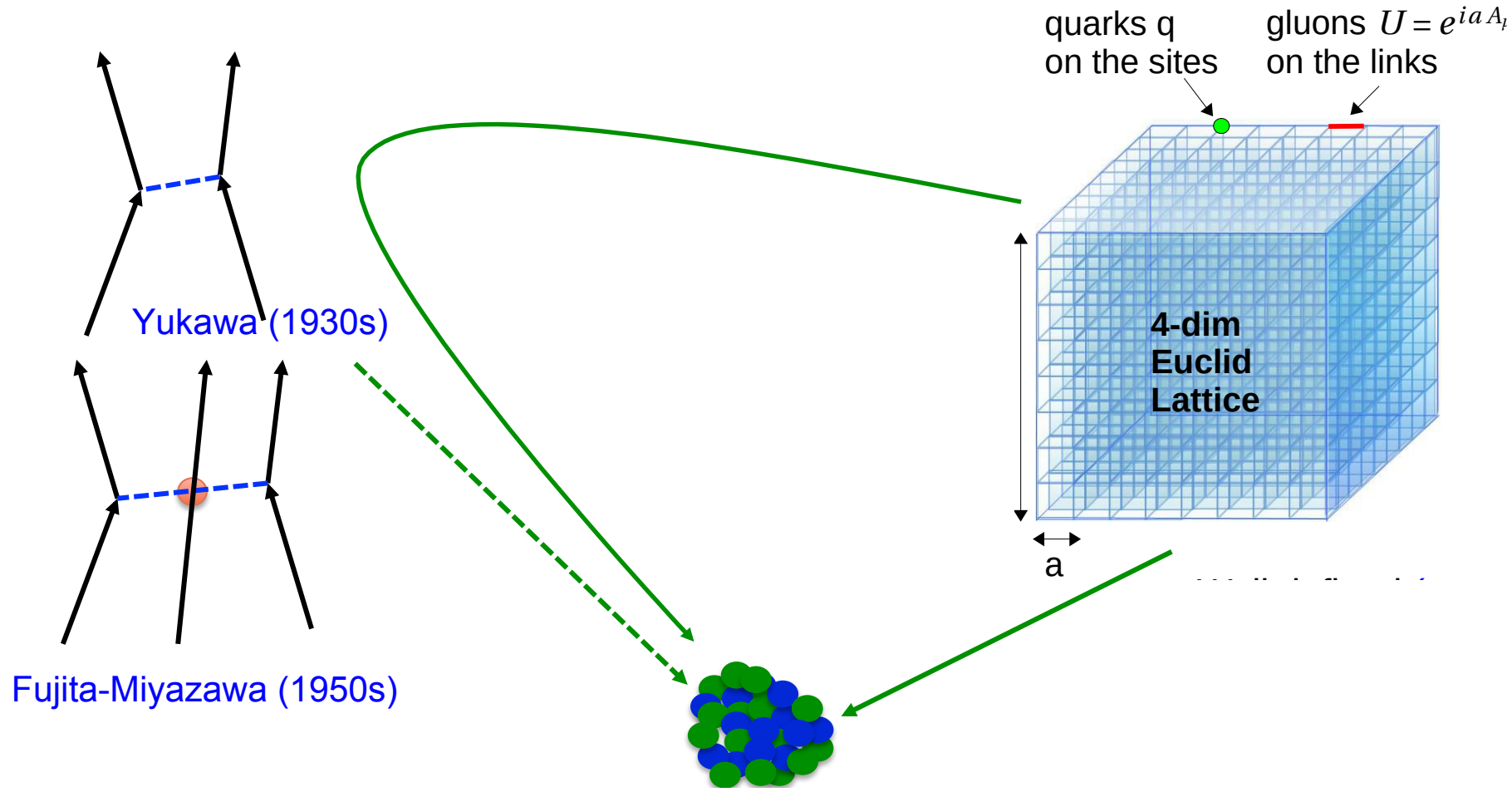

Why nuclear interactions on the Lattice??

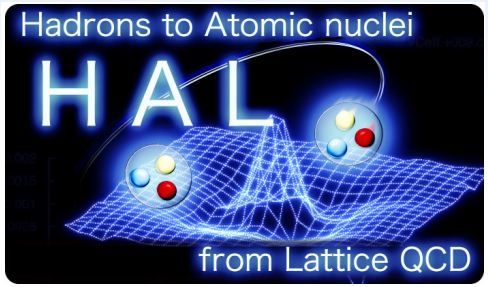

- *Extend LQCD beyond few-bodies*
- *Not based on a specific EFT momentum scale*
  ➔ exploitable to high densities (e.g. Neutron stars)
- *No LECs to worry about ...but:*
- *Variation in potentials from variation in sink operators (➔ estimation of theoretical uncertainties)*
- *Direct derivation of hyperon-nucleon interactions*
- *3NF can be derived consistently with NN interactions*

➔ *Need to develop appropriate many-body methods*

Two-Nucleon HAL potentials

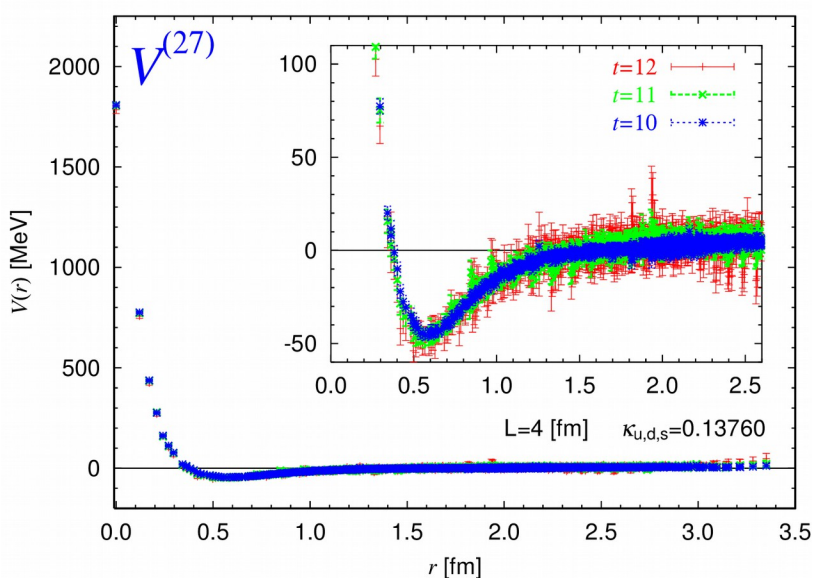

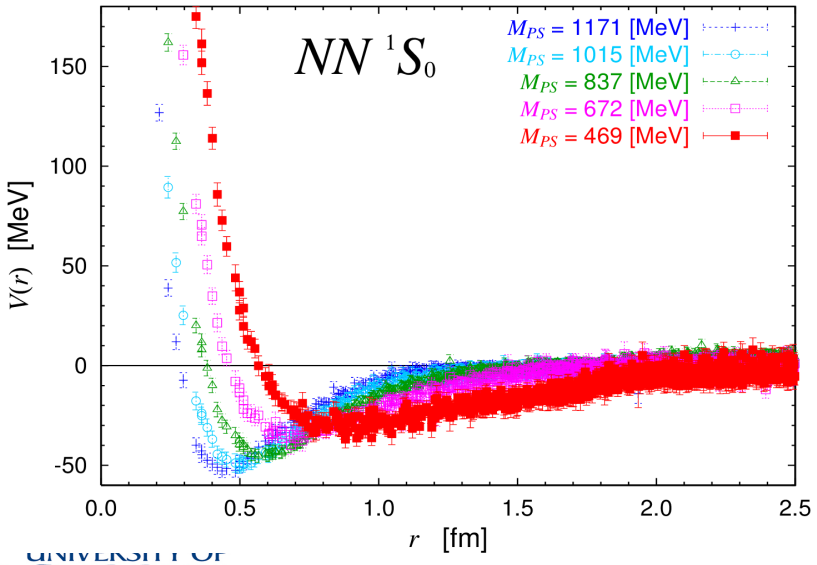

Quark mass dependence of *V(r)* for NN partial wave ($^1S_0$, $^3S_1$, $^3S_1$-$^3D_1$)

➔ Potentials become stronger m_π as decreases.

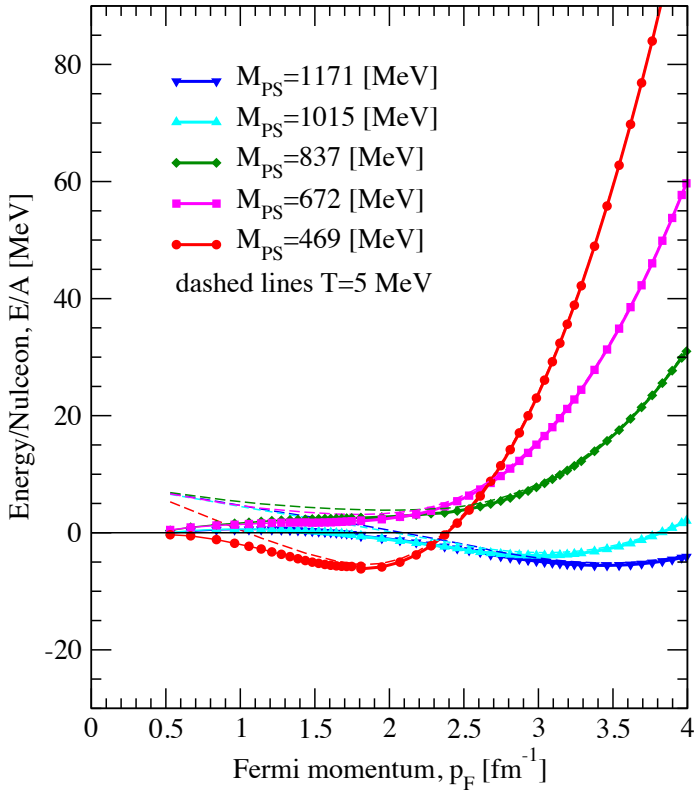

T. Inoue *et al.*,
Phys. Rev. Lett. **111** 112503 (2013).

UNIVERSITY OF SURREY

Prog. Theor. Exp. Phys. 01A105 (2012)

(Finite-T results by A. Carbone, priv. comm.)

Analysis of Brueckner HF

Scattering of two nucleons outside the Fermi sea (➔BHF):

$$G(\omega) = V + \int dk_a dk_b V \frac{\hat{Q}}{\omega - \varepsilon(k_a) - \varepsilon(k_b) + i\eta} G(\omega)$$

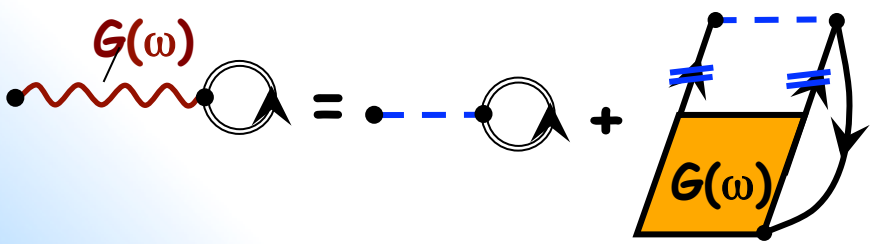

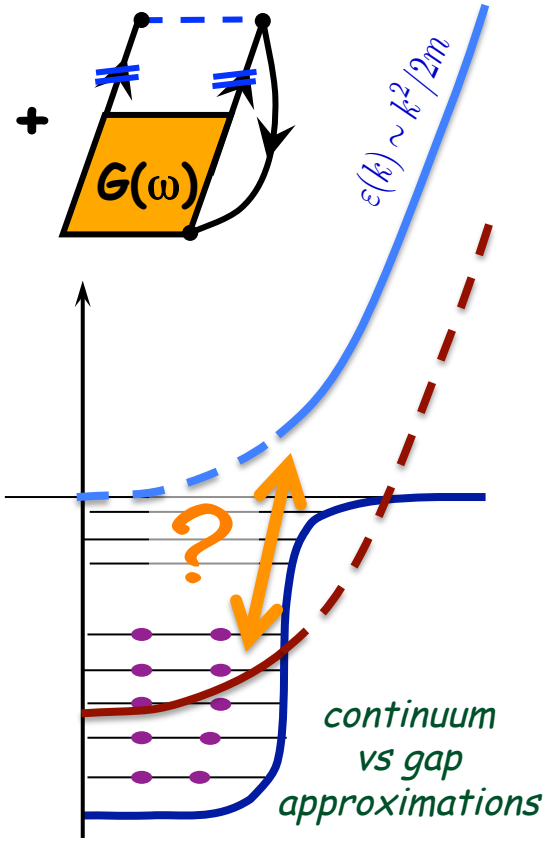

Mixed SCGF-Brueckner approach

Solve full many-body dynamics in model space (P+Q') and the Goldstone's ladders outside it (i.e. in Q'' only):

$$G''(\omega) = V + \int dk_a dk_b V \frac{\hat{Q}''}{\omega - \varepsilon(k_a) - \varepsilon(k_b) + i\eta} G''(\omega)$$

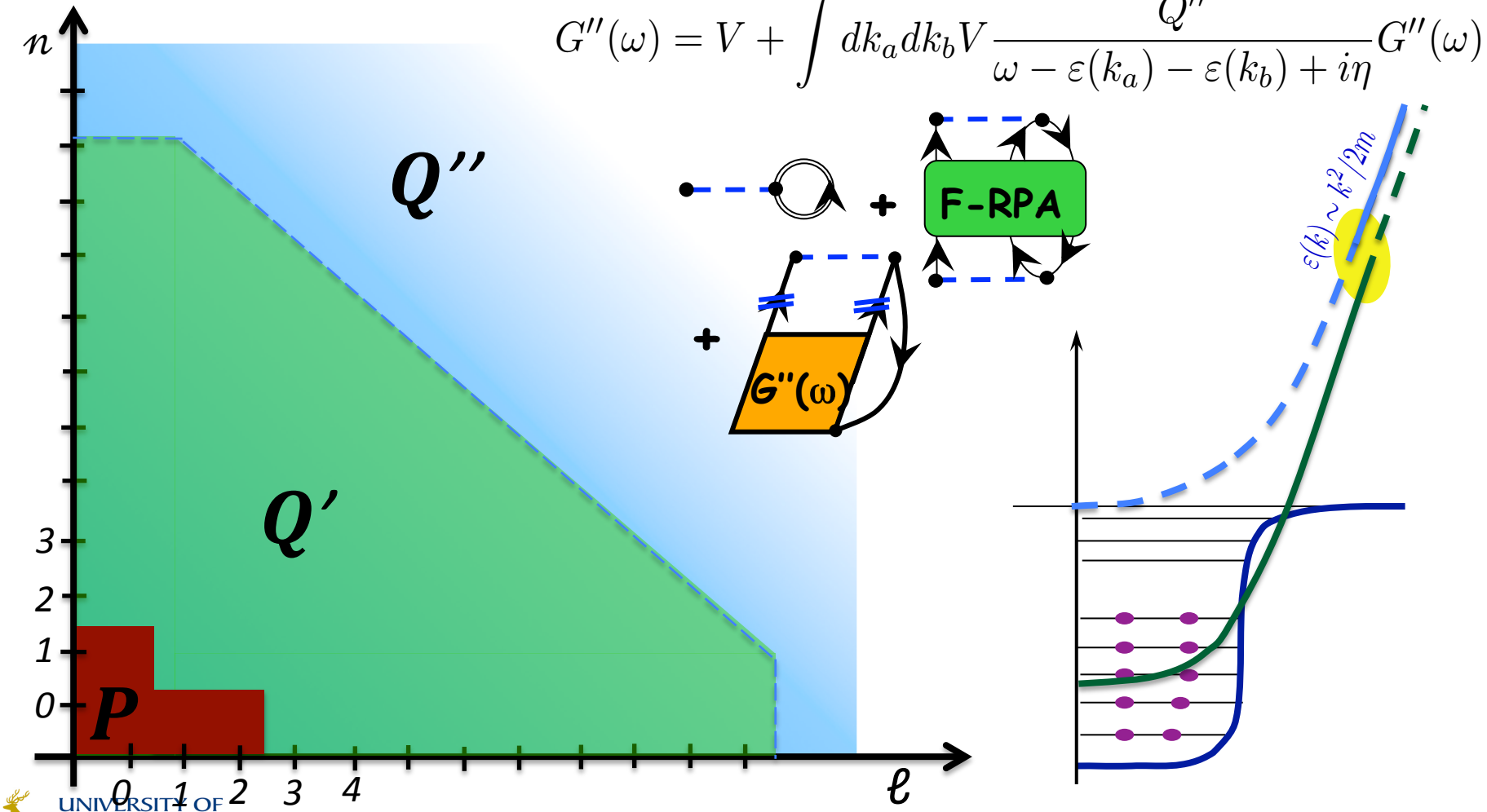

Treating short-range corr. with a G-matrix

- The short-range core can be treated by summing ladders outside the model space:

$$\Sigma^{\mathrm{MF}}_{\alpha\beta}(\omega) = i\sum_{\gamma\delta}\int \frac{d\omega'}{2\pi} G_{\alpha\gamma,\delta\beta}(\omega+\omega')g_{\delta\gamma}(\omega')$$

=

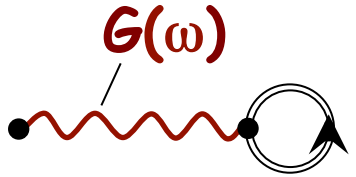

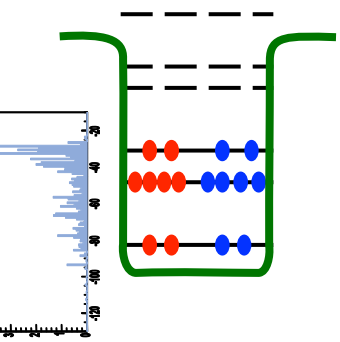

$$\Sigma^{\star}(\mathbf{r},\mathbf{r}';\omega) = \Sigma^{MF}(\mathbf{r},\mathbf{r}';\omega) + \tilde{\Sigma}(\mathbf{r},\mathbf{r}';\omega)\ .$$

$$Z_\alpha = \int d\mathbf{r}\ |\psi^{A\pm1}_\alpha(\mathbf{r})|^2 = \left.\frac{1}{1-\dfrac{\partial\Sigma^{\star}_{\hat{\alpha}\hat{\alpha}}(\omega)}{\partial\omega}}\right|_{\omega=\pm(E^{A\pm1}_\alpha - E^{A}_0)}$$

Two contributions to the derivative:

- $\Sigma^{\mathrm{MF}}_{\alpha\beta}(\omega)$ is due to scattering to (high-k) states in the Q space
- $\Sigma(\mathbf{r},\mathbf{r}';\omega)$ accounts for low-energy (long range) correlations

(Galitskii-Migdal-Boffi-) Koltun sumrule

- Koltun sum rule (with NNN interactions):

$$\sum_\alpha \frac{1}{\pi}\int_{-\infty}^{\epsilon_F} d\omega\,\omega\,\mathrm{Im}\,G_{\alpha\alpha}(\omega) = \langle\Psi_0^N|\hat{T}|\Psi_0^N\rangle + 2\langle\Psi_0^N|\hat{V}|\Psi_0^N\rangle + 3\langle\Psi_0^N|\hat{W}|\Psi_0^N\rangle$$

two-body

three-body

$$E_0^N = \frac{1}{2\pi}\int_{-\infty}^{\epsilon_F} \mathrm{d}\omega \sum_{\alpha\beta}(T_{\alpha\beta}+\omega\delta_{\alpha\beta})\mathrm{Im}\,G_{\beta\alpha}(\omega) - \frac{1}{2}\langle\Psi_0^N|\widehat{W}|\Psi_0^N\rangle$$

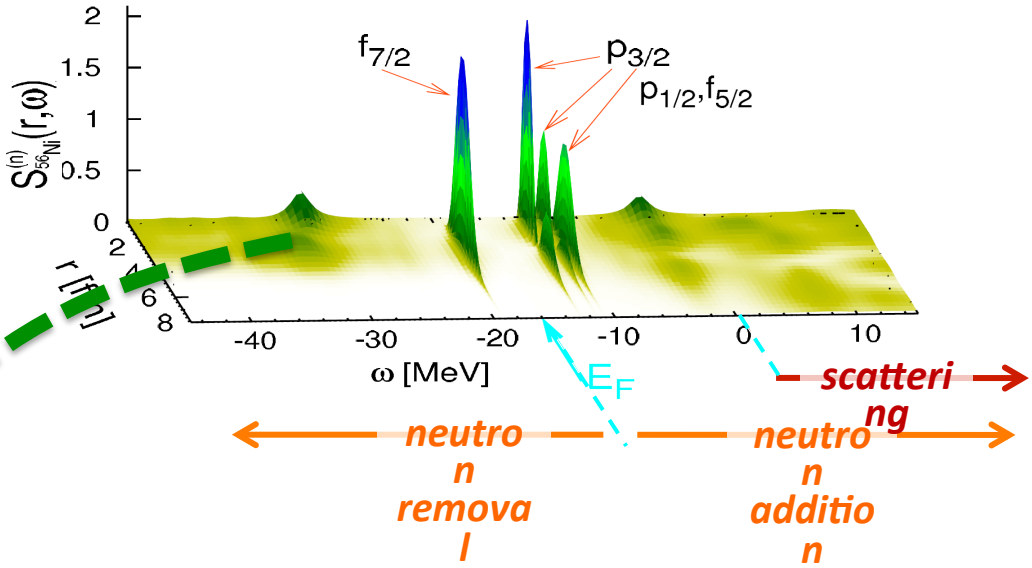

High-k and missing energy tail from SRC… (currently neglected in calculating Koltun SR)

Benchmark on ^{4}He

C. McIlroy, CB, et al., arXiv:1701.02607 [nucl-th]

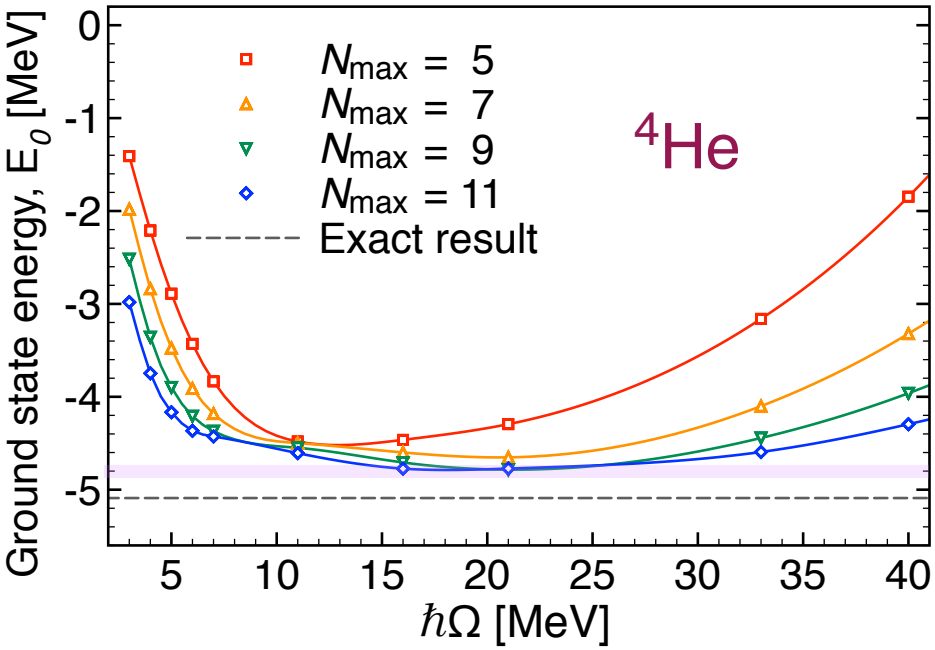

Can benchmark the Gmtx+ADC(3) method on light ^{4}He, where exact solutions are possible:

	G(ω) + ADC(3)	Exact
HALQCD @ $m_\pi \approx 470$MeV	4.79(3) MeV	5.09 MeV[1]

[1]H. Nemura *et al.*, Int. J. Mod. Phys. E **23**, 1461006 (2014)

➔ *Can expect accuracy on binding energies at about 10%*

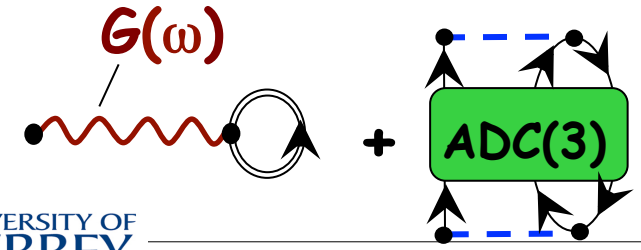

$$G''(\omega) = V + \int dk_a dk_b V \frac{\hat{Q}''}{\omega - \varepsilon(k_a) - \varepsilon(k_b) + i\eta} G''(\omega)$$

Binding of ^{16}O and ^{40}Ca:

C. McIlroy, CB, et al., arXiv:1701.02607 [nucl-th]

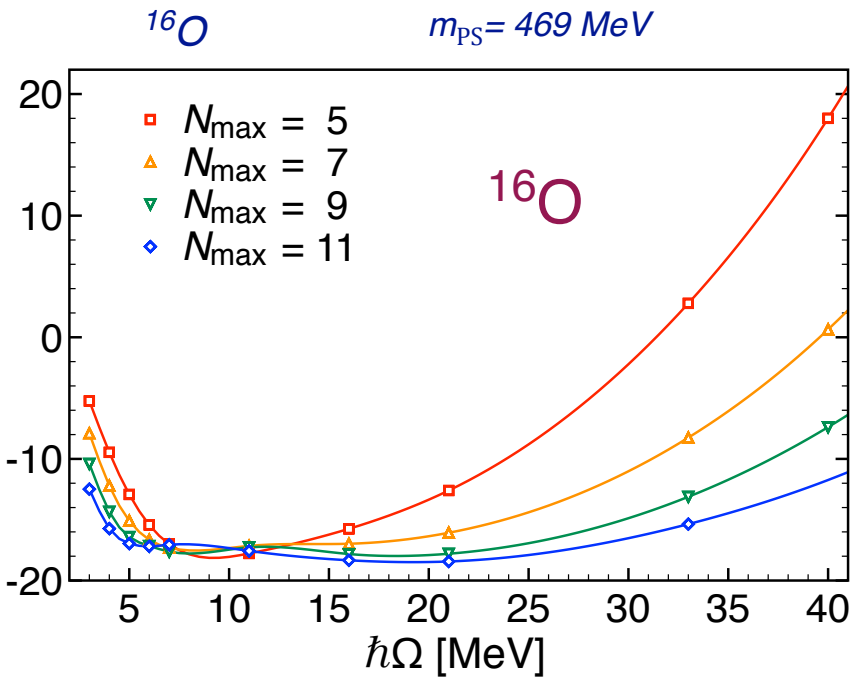

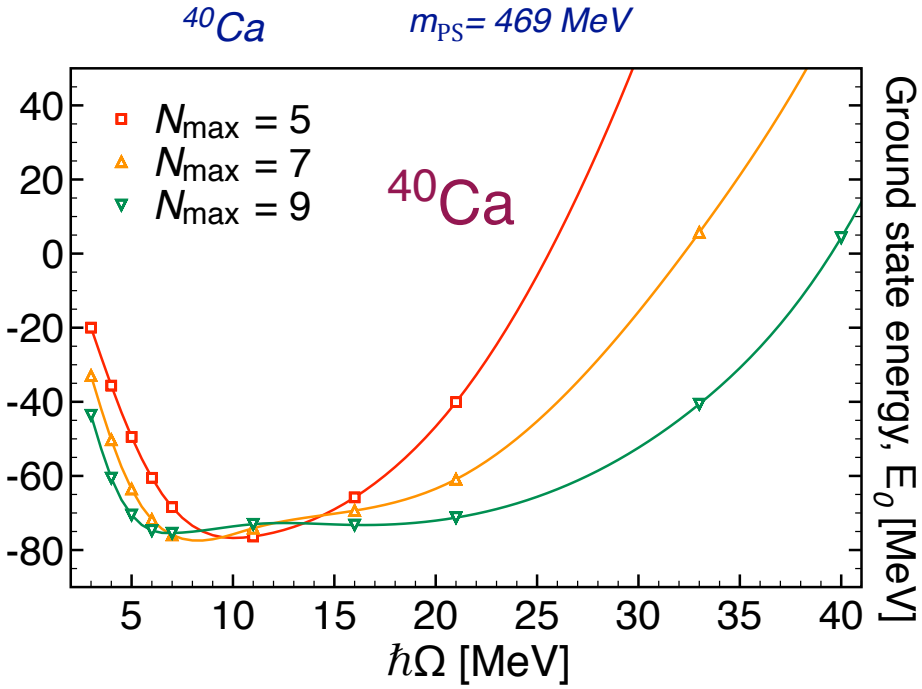

Binding energies are ~17 MeV ^{16}O and 70-75MeV for ^{40}Ca. Possibly being underestimated by 10%

➔ ^{16}O at $m_\pi \approx 470$ MeV is unstable toward 4-α breakup*!*

E_0^A [MeV]	^{4}He	^{16}O	^{40}Ca
BHF [22]	-8.1	-34.7	-112.7
G(ω) + ADC(3)	-4.80(0.03)	-17.9 (0.3) (1.8)	-75.4 (6.7) (7.5)
Exact Result [51]	-5.09	–	–
Separation into ^{4}He clusters:		-2.46 (0.3) (1.8)	24.5 (6.7) (7.5)

[C.S.McIlroy, CB, HAL coll., in prep]

Infrared convergence

Moore et al., Phy. Rev. C**87**, 044326 (2013)

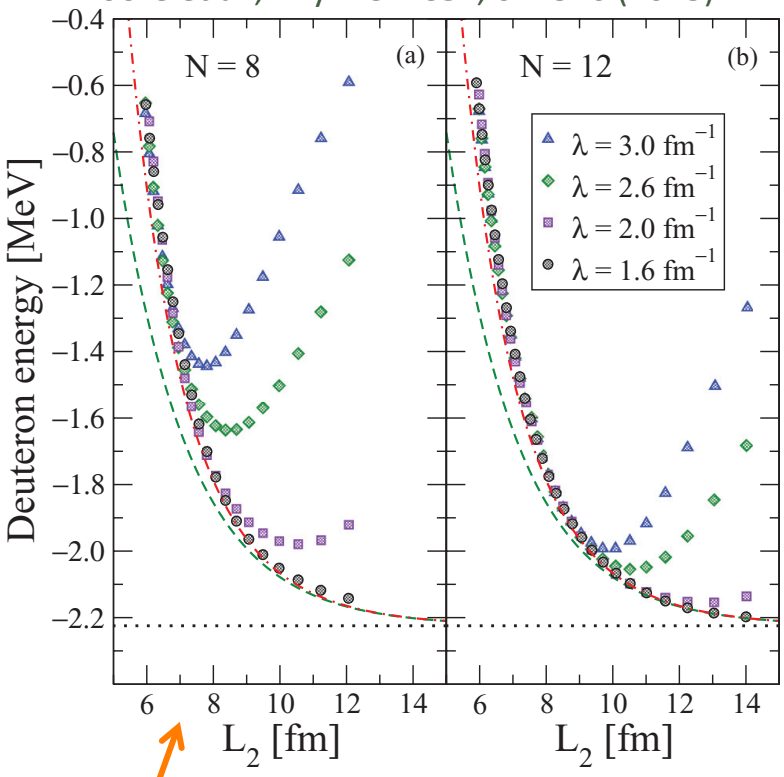

Deuteron g.s. Energy
EM(500) – N3LO two-nucleon force

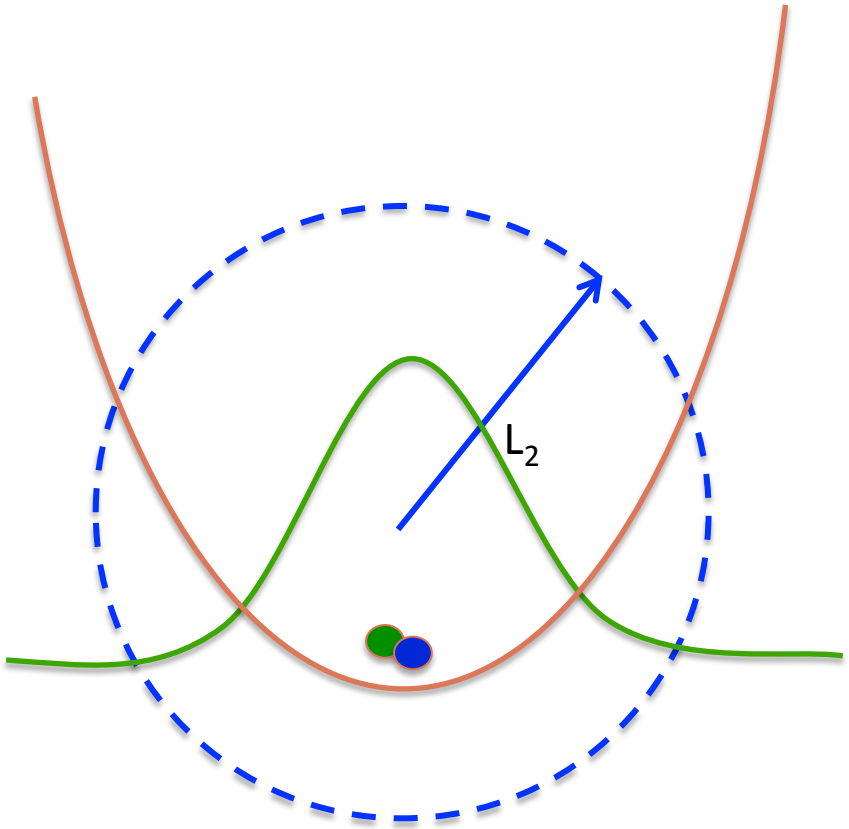

$$L_2 = \sqrt{2(N + 3/2 + 2)}b$$

Infrared convergence

Moore et al., Phy. Rev. C**87**, 044326 (2013)

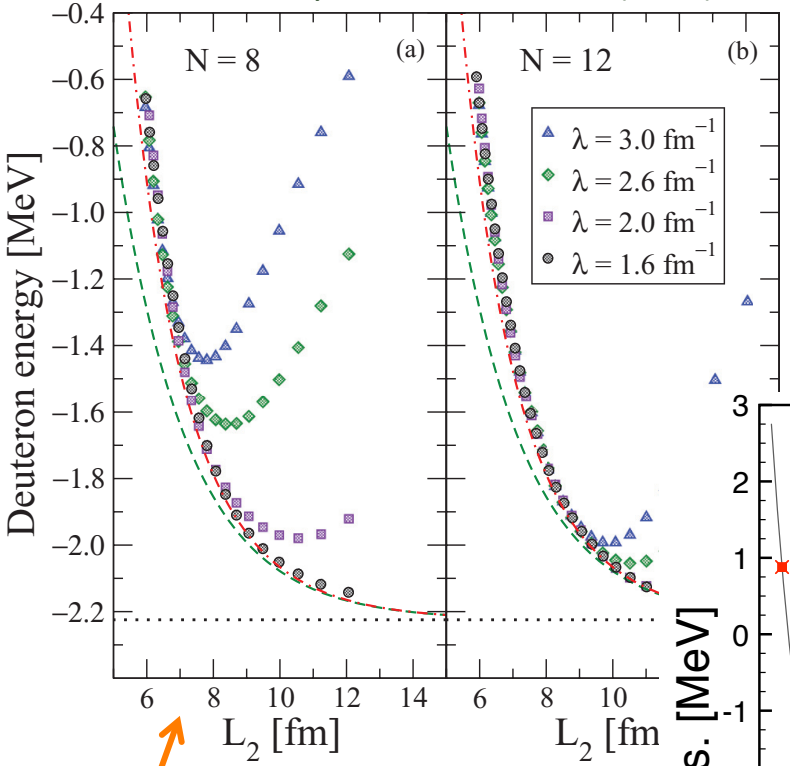

Deuteron g.s. Energy
EM(500) – N3LO two-nuc

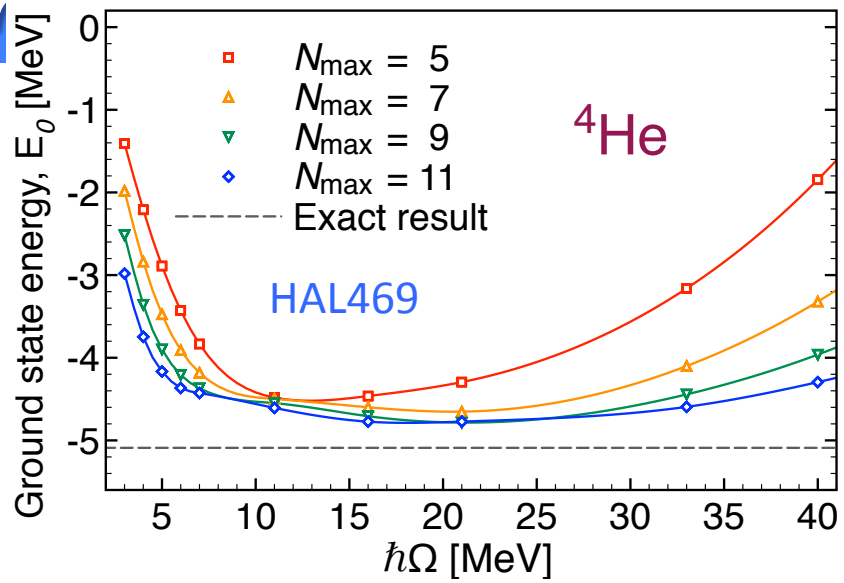

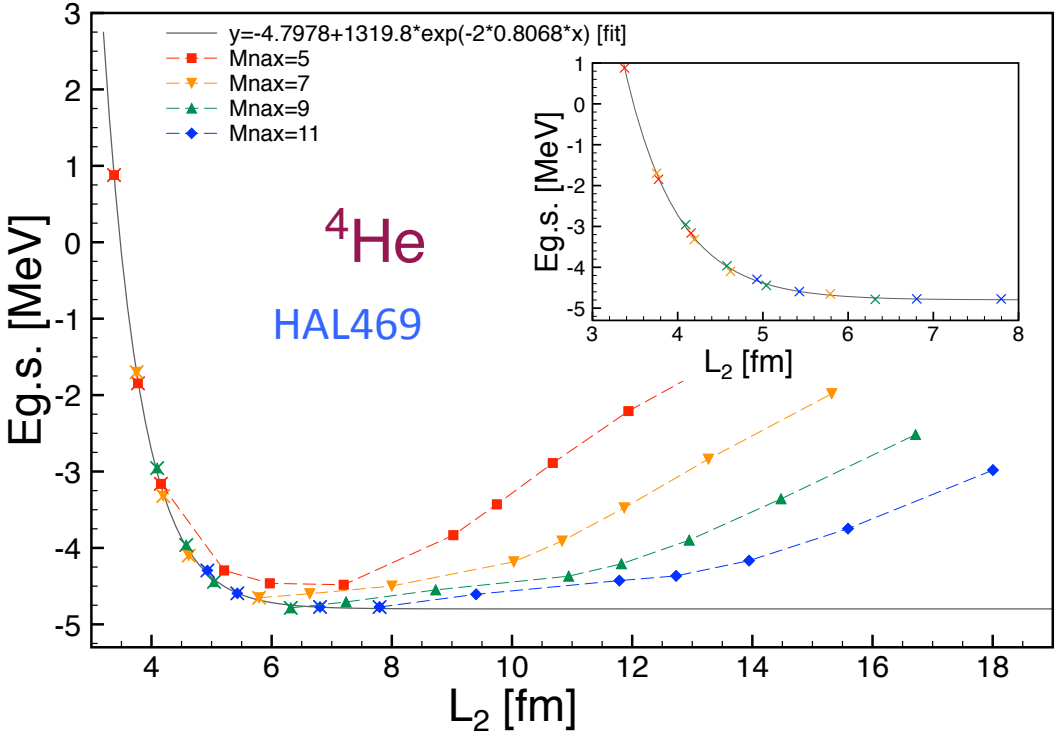

Results for binding

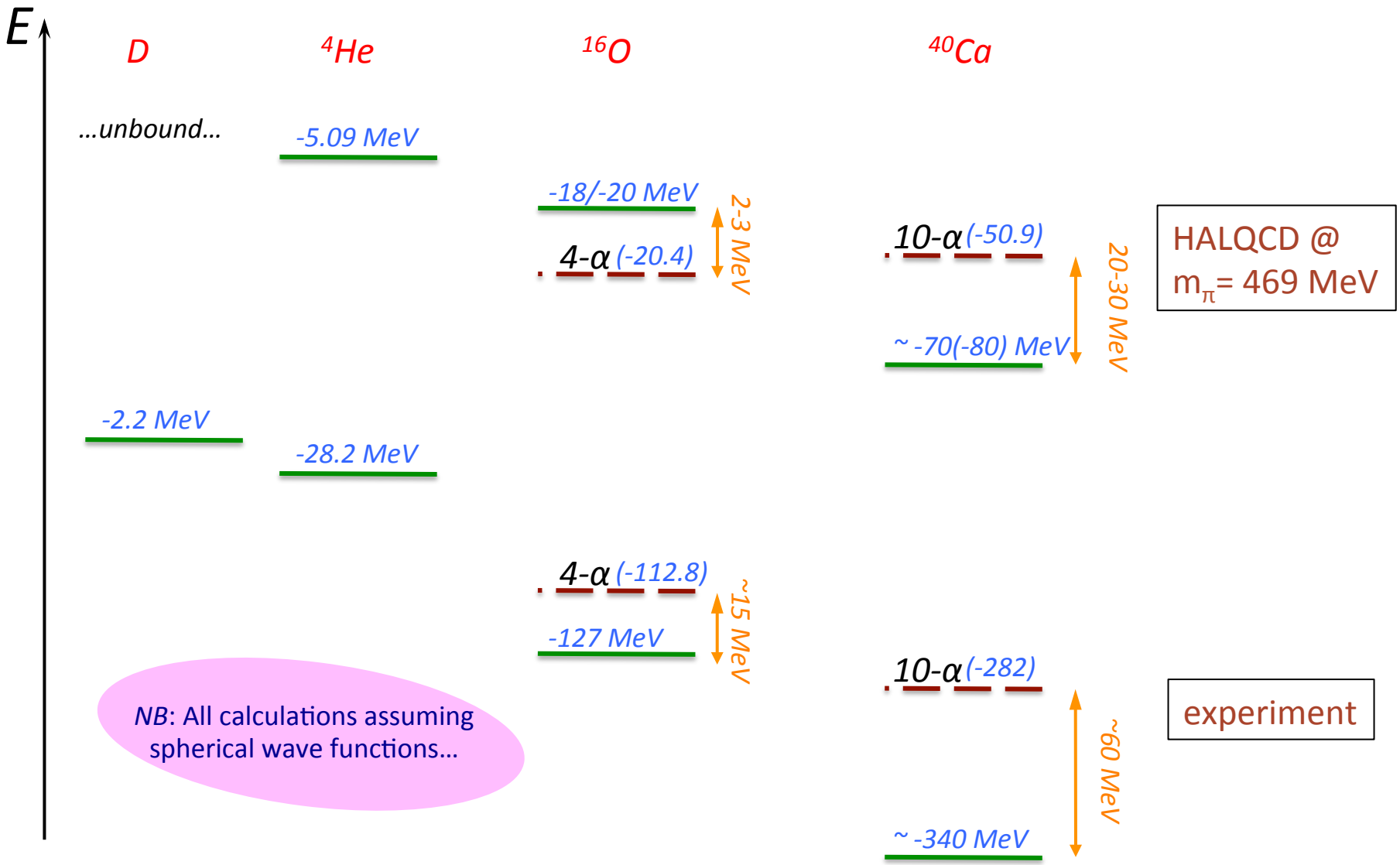

C. McIlroy, CB, et al., arXiv:1701.02607 [nucl-th]

Matter distribution of ^{16}O and ^{40}Ca:

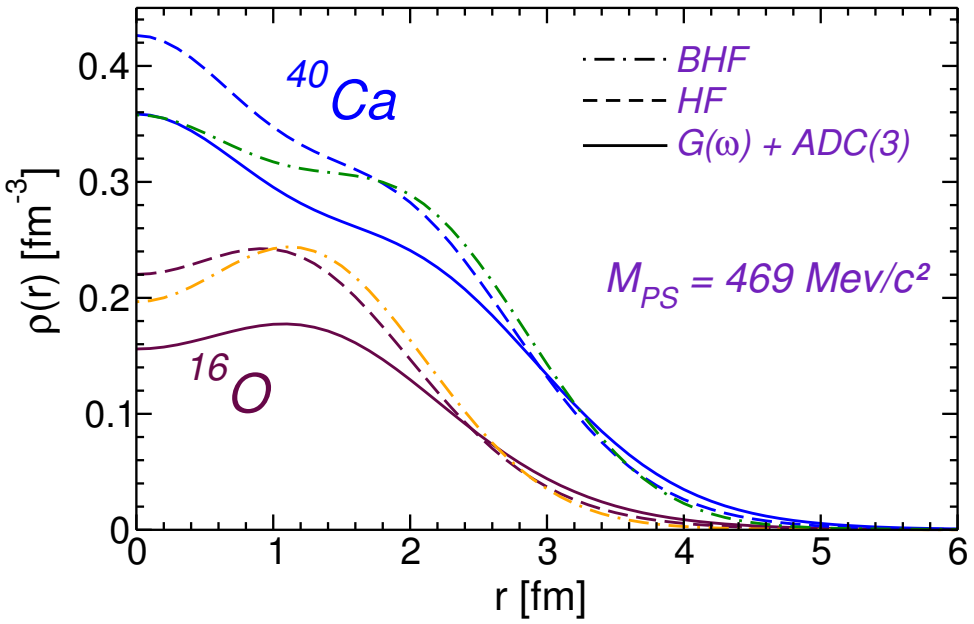

Calculated matter radii at $m_\pi \approx 470$ MeV:

		^{16}O	^{40}Ca
$r_{pt-matter}$:	BHF [22]	2.35 fm	2.78 fm
	HF	2.39 fm	2.78 fm
	G(ω) + ADC(3)	2.64 fm	2.97 fm
r_{charge}:	G(ω) + ADC(3)	2.77 fm	3.08 fm
	Experiment [54, 55]	2.73 fm	3.48 fm

C. McIlroy, CB, et al., arXiv:1701.02607 [nucl-th]

Spectral strength in ^{16}O and ^{40}Ca:

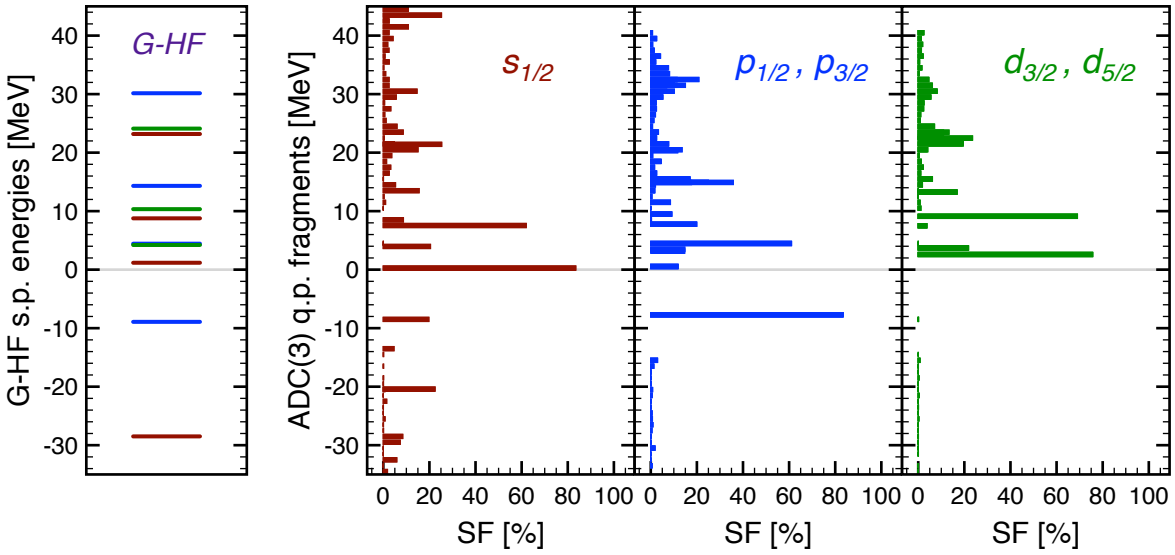

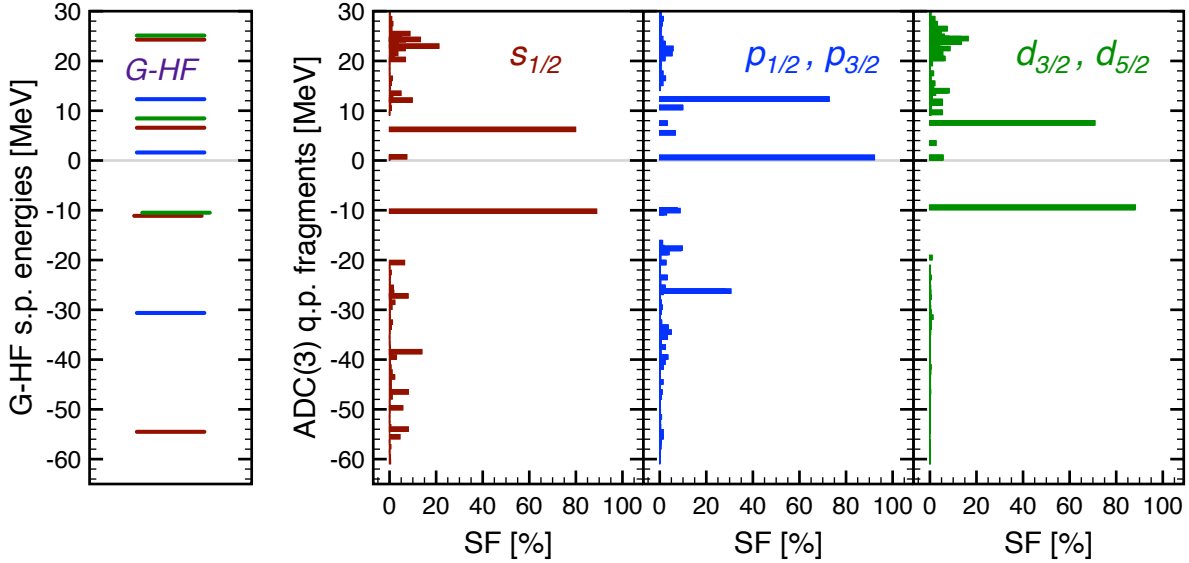

Particle-hole gaps:

^{16}O

m_π= 469 MeV: ~8 MeV

Expt (phys m_π): 11.5 MeV

^{40}Ca

m_π= 469 MeV: ~10 MeV

Expt (phys m_π): 7.5 MeV

UNIVERSITY OF SURREY

C. McIlroy, CB, et al., arXiv:1701.02607 [nucl-th]

Spectral strength in ^{16}O and ^{40}Ca:

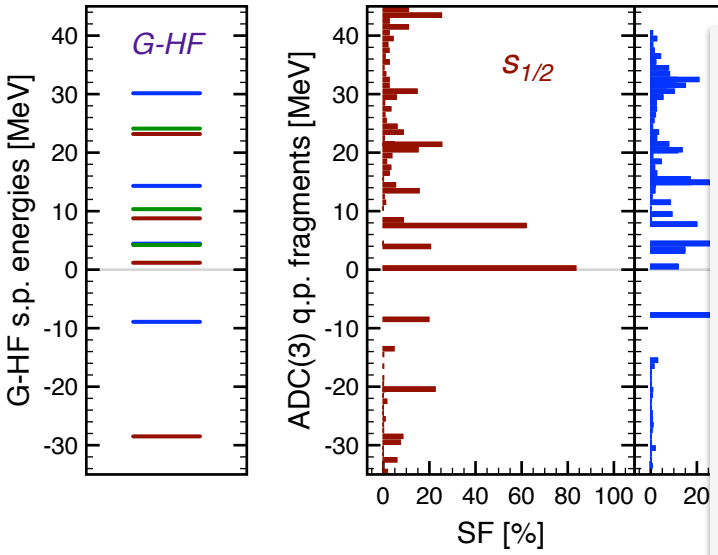

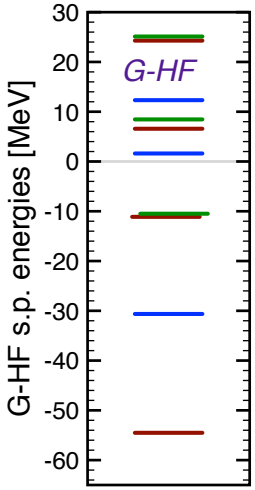

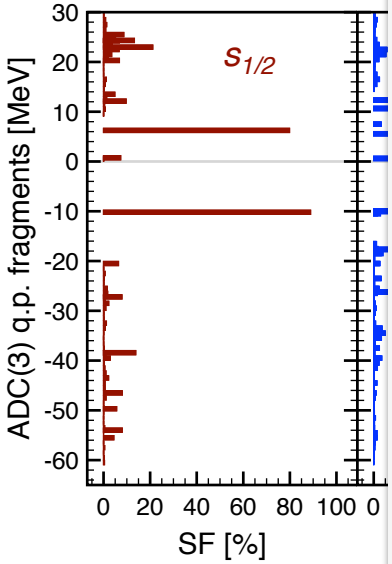

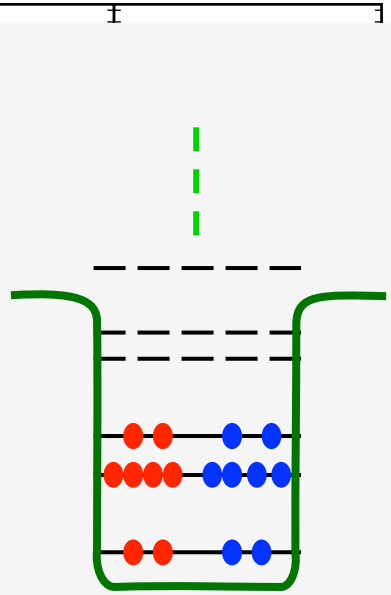

independent particle picture?

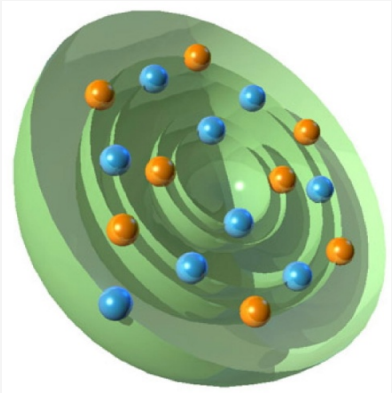

C. McIlroy, CB, et al., arXiv:1701.02607 [nucl-th]

Future application for Ys in nuclei now possible

- Physical mass now under reach ($m_\pi \approx 145$ MeV) for hyperons
- Need to improve on statistic for the NN sector

$\Omega\Omega$ potential

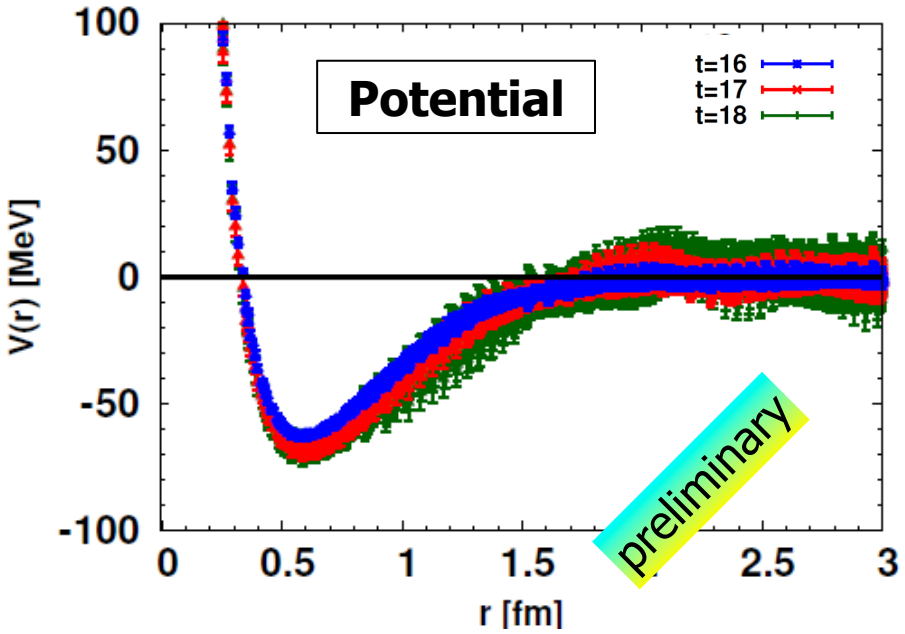

$NN(^3S_1)$ tensor potential

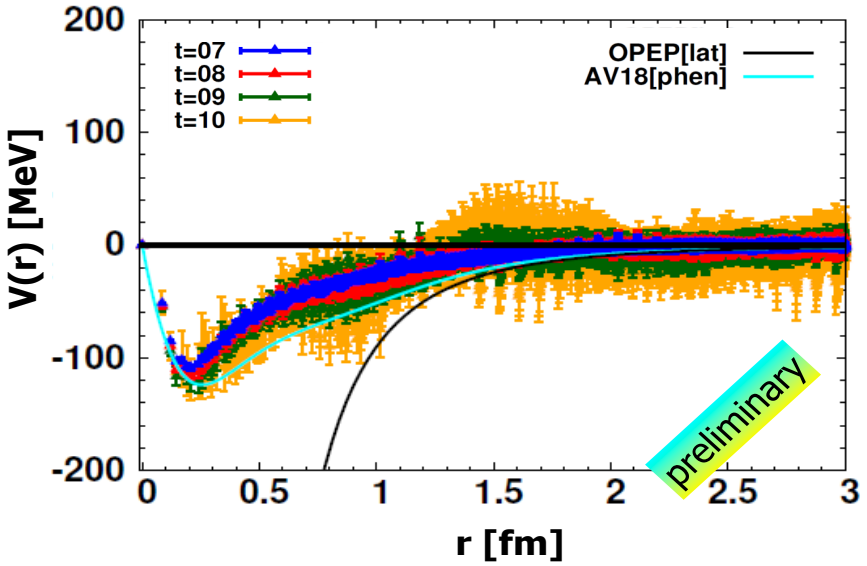

HALQCD coll. -- Talk of ***S. Aoki*** at Kavli institute, Oct. 2016

Summary

Thank you for your attention!!!

Mid-masses and chiral interactions:

- → *Leading order 3NF are crucial to predict many important features that are observed experimentally (drip lines, saturation, orbit evolution, etc…)*
- → *Experimental binding is predicted accurately up to the lower sd shell (A≈30) but deteriorates for medium mass isotopes (Ca and above) with roughly 1 MeV/A over binding.*
- → *New fits of chiral interaction are promising for low-energy observables and for scattering (see A. Idini, next).*

HALQCD Nuclear forces:

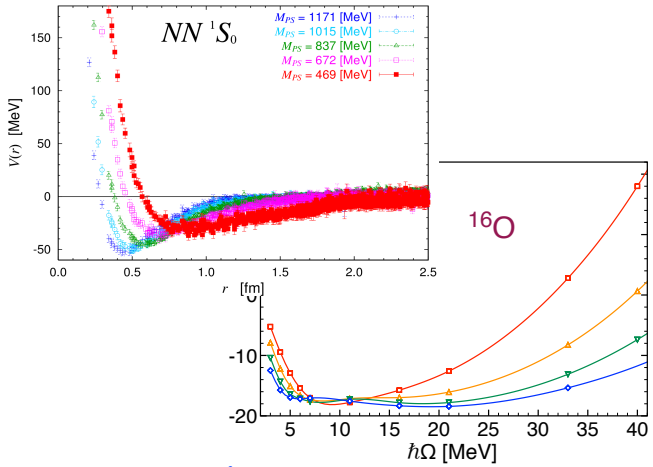

- → *Strong short range behavior calls for new ideas in ab-initio many-body methods. Diagram resummation through G-matrix is good starting point (to be extended)*
- → *At m_π=469MeV, closed shell 4He, 16O and 40Ca are bound. But oxygen is unstable toward 4-α break up, calcium stays bound. Underestimation of radii increases with A do to large saturation density (as for EM(500)+NLO3NF).*

Collaborators

UNIVERSITY OF SURREY

A. Cipollone, *C. McIlroy*
A. Rios, A. Idini, F. Raimondi

Universitat de Barcelona

A. Polls

cea
energie atomique • energies alternatives

V. Somà, T. Duguet

Washington University in St. Louis

W.H. Dickhoff, S. Waldecker

EMMI

TECHNISCHE UNIVERSITÄT DARMSTADT

A. Carbone

Center for Molecular Modeling

D. Van Neck,

TRIUMF

P. Navratil

M. Hjorth-Jensen

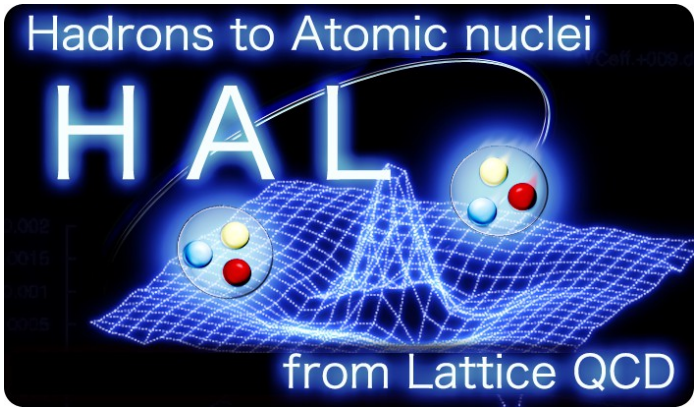

S. Aoki,	YITP Kyoto Univ.
T. Doi, **T. Hatsuda**, Y. Ikeda,	RIKEN Nishina
T. Inoue,	Nihon Univ.
N. Ishii, K. Murano,	RCNP Osaka Univ
H. Nemura, K. Sasaki	Univ. Tsukuba
F. Etminan	Univ. Birjand
T. Miyamoto,	Univ. Tsukuba
T. Iritani	Stony Brook Univ.
S. Gongyo	YITP Kyoto Univ.